12-1997

Investigation of isolated sand shoals on the inner shelf of Virginia relative to the potential for aggregate mining : report on study of possible wave force alternations on the proposed dredging at Sandbridge Shoal, VA

Jerome Y.-P. Maa
Virginia Institute of Marine Science

Carl H. Hobbs III
Virginia Institute of Marine Science

REPORT ON

Study of Possible Wave Force Alternations on the Proposed Dredging at Sandbridge Shoal, VA

U. S. Minerals Management Service - Commonwealth of Virginia
Cooperative Project

INVESTIGATION OF ISOLATED SAND SHOALS ON THE INNER SHELF OF VIRGINIA RELATIVE TO THE POTENTIAL FOR AGGREGATE MINING

Submitted to

U. S. Department of the Interior
Minerals Management Service
Office of International and Marine Minerals
381 Elden Street
Herndon, Virginia 22070-4817

by

School of Marine Science
Virginia Institute of Marine Science
College of William & Mary
P. O. Box 1346
Gloucester Point, Virginia 23062-1346

Jerome P.-Y. Maa
Principal Investigator

Carl H. Hobbs, III
Project Manager

December 1997

REPORT ON

Study of Possible Wave Force Alternations on the Proposed Dredging at Sandbridge Shoal, VA

U. S. Minerals Management Service - Commonwealth of Virginia
Cooperative Project

INVESTIGATION OF ISOLATED SAND SHOALS ON THE INNER SHELF OF VIRGINIA RELATIVE TO THE POTENTIAL FOR AGGREGATE MINING

Submitted to

U. S. Department of the Interior
Minerals Management Service
Office of International and Marine Minerals
381 Elden Street
Herndon, Virginia 22070-4817

by

School of Marine Science
Virginia Institute of Marine Science
College of William & Mary
P. O. Box 1346
Gloucester Point, Virginia 23062-1346

Jerome P.-Y. Maa
Principal Investigator

Carl H. Hobbs, III
Project Manager

December 1997

TABLE OF CONTENTS

INTRODUCTION

The Virginia Institute of Marine Science, together with other state agencies, has a continuing interest in preserving the coastline of Virginia, particularly, the Atlantic coastline in the vicinity of the resort city of Virginia Beach. Because a well maintained beach can serve several purposes, *e.g.*, (1) providing public recreational areas, (2) protecting valuable properties that are located near coastline, and (3) reducing the rate of land loss, a great deal of efforts has been devoted to understand the processes that affect the change of shoreline. Among several erosion forces, waves are especially important elements as they can alter the shoreline significantly.

One may use any of several approaches to maintain a beach properly, and perhaps may use all available approaches in parallel to obtain the best results. In the coastal sector of Virginia Beach, beach nourishment using material from inland borrow pits has been done constantly during the last two decades. It has become more difficult to find land sources of good beach-quality sand. Sand loss from the beach due to both shore normal and longshore transport creates the need to find a reliable source of good quality sand for future use.

Sandbridge Shoal (Fig. 1) located approximately 20 miles south of Virginia Beach and 3 miles offshore, has been identified as a potential source of good beach-quality sand (Kimball and Dame, 1989). Use of the sand resources there, however, causes a great deal of concern that dredging may result in severe beach erosion at Sandbridge due to alternation of the wave transformation process.

Understanding the possible changes to the shoreline due to dredging at the shoal requires a comprehensive understanding of the wave climate, the wave transformation process, and the associated shoreline responses.

In our earlier studies (Maa, 1995; Maa and Hobbs, in press) we assumed that the sand taken from Sandbridge Shoal for the first few years would be limited to around 10^6 m^3. Our results indicated that this amount of sand mining would cause only marginal changes (5%) to the long period waves in the worst scenario (Maa and Hobbs, in press). Since that study, sand has been mined from Sandbridge Shoal and placed along the beach at Dam Neck, immediately north of Sandbridge. Because of the rapid growth of demand for beach-quality sand and the as yet unsuccessful effort to find other sand sources, there is a great need to study what possibly would happen if there were extensive sand mining at Sandbridge Shoal , up to 2×10^7 m^3 during the next 10 years or even 20 years. In this study, we addressed this concern by examining the possible major dredging at Sandbridge Shoal and studying the wave transformation process. The following are results from this study.

For completeness, results of previous studies are summarized here. Details may be found in those reports (Maa, 1995; Maa and Hobbs, in press).

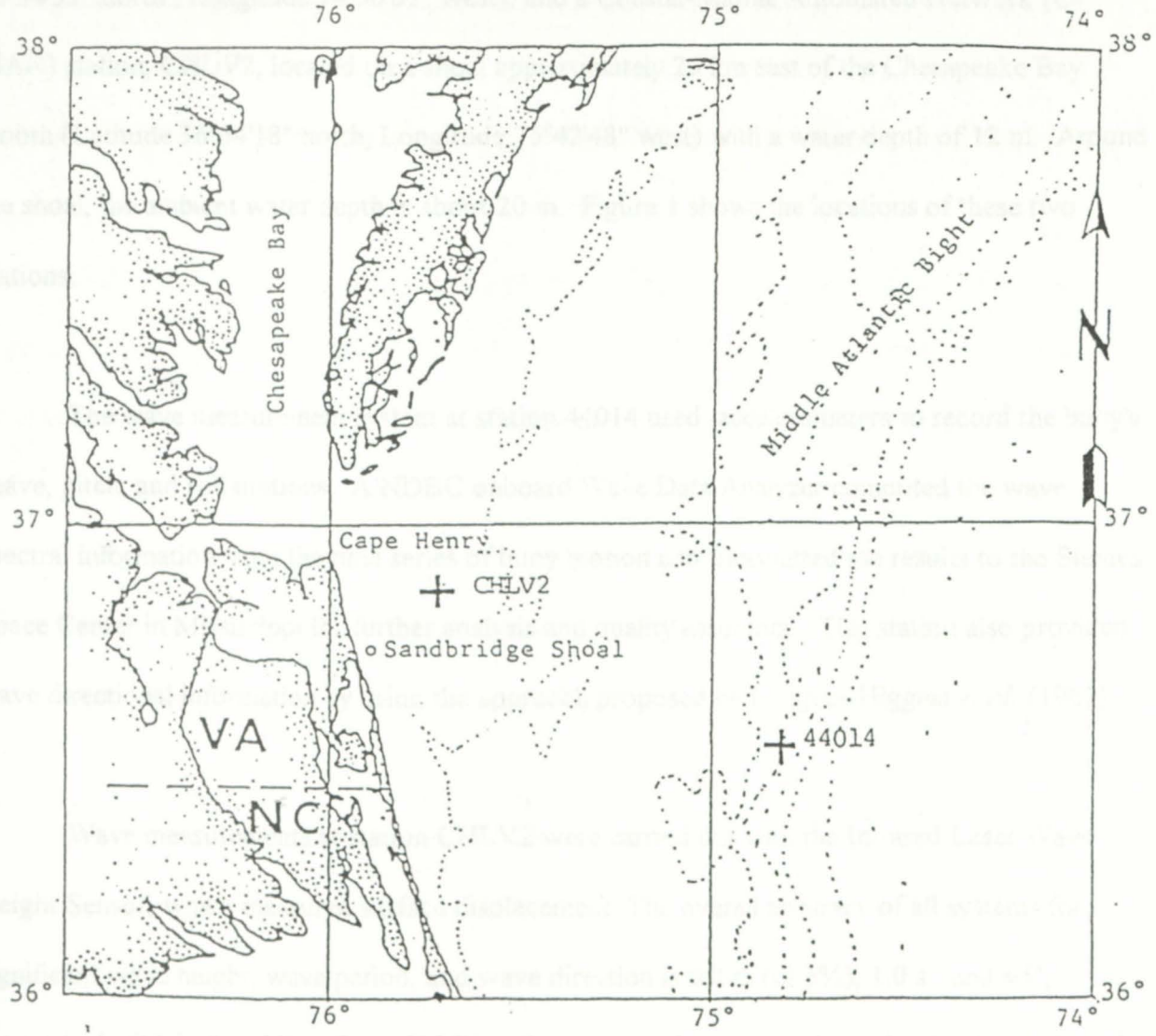

Fig. 1. Location Map of Wave Stations and Study Area

WAVE DATA

The National Data Buoy Center (NDBC) has two stations in the study area: A moored buoy station, 44014, located near the continental shelf break with a water depth of 48 m (Latitude 36°34'59 "north , Longitude 74°50'01" west), and a Coastal-Marine Automated Network (C-MAN) station, CHLV2, located on a shoal approximately 25 km east of the Chesapeake Bay mouth (Latitude 36°54'18" north, Longitude 75°42'48" west) with a water depth of 12 m. Around the shoal, the ambient water depth is about 20 m. Figure 1 shows the locations of these two stations.

The wave measurement system at station 44014 used accelerometers to record the buoy's heave, pitch, and roll motions. A NDBC onboard Wave Data Analyzer computed the wave spectral information from the time series of buoy motion and transmitted the results to the Stennis Space Center in Mississippi for further analysis and quality assurance. This station also provided wave directional information by using the approach proposed by Longuet-Higgins *et al.* (1963).

Wave measurements at station CHLV2 were carried out with the Infrared Laser Wave Height Sensor, which measured surface displacement. The overall accuracy of all systems for significant wave height, wave period, and wave direction is 0.2 m (or 5%), 1.0 s., and ±5°, respectively (Meindl and Hamilton, 1992). All processed data were achieved in National Oceanic Data Center (NODC) in Washington, D.C. using a special ASCII format. These data were stored in CD-ROM and are easily retrieved. We developed computer software to analyze the data and store the basic information such as date, time, significant wave heights, zero cross periods, peak

energy wave periods, and wave spectrum information on separate disk files for later use.

Statistical Analysis

The joint distribution of significant wave height and peak energy wave period for the two stations were analyzed in the earlier study. The distribution of recorded significant wave height and peak energy period indicate the relative abundance of each wave height and period (Fig. 2).

Table 1 shows the maximum significant wave heights that occurred during each of the 7 years. The recorded maximum significant wave height (6.2 m with a peak wave period of 20 seconds, occurred on 9/27/85) probably qualifies as the most severe storm wave.

Table 1

Observed Maximum Waves

Date	Time	H_significant (m)	T_Peak (sec)
9/27/85	10:00	6.2	20
12/02/86	21:00	4.2	10
3/10/87	15:00	4.5	10
2/19/88	20:00	3.3	5.6
2/24/89	22:00	4.9	12.5
10/26/90	17:00	4.0	10
11/10/91	03:00	4.6	10
1/04/92	11:00	4.9	14.3

Model Waves

Based on the measurements at station CHLV2 and Table 1, we identified the following three wave conditions (Table 2) to use in modeling the possible changes due to dredging at the Sandbridge Shoal.

Table 2

Selected Model Waves

Wave Height (m)	Wave Period (sec)	Remark
6.2	20	The most severe sea
3.0	14	Severe sea
1.9	12	Northeaster

Wave Direction

Wave directional information is only available for station 44014. In our previous study, we analyzed the information acquired at this station and presented the following figures (Figs. 3 and 4) to show the directional distribution for wave height and wave period. The orientation of the shoreline at Sandbridge is plotted as a reference. Figure 3 indicates that directional distribution of wave height is relatively uniform from SSE to NNE and that the most common wave direction is ESE. The waves coming from NNE to ENE are mainly large waves caused by Northeasters. Their periods, however, are not long except the ENE direction. Most of the waves from the NNE and NE are less than 8 sec. Long period waves mainly came from ENE and E because of the long fetch. Thus, waves coming from the ENE are most important because of the possible large wave height and long period. Waves coming from the ESE to SSE directions any wave height but their wave periods are rather short. Considering that the water depth at

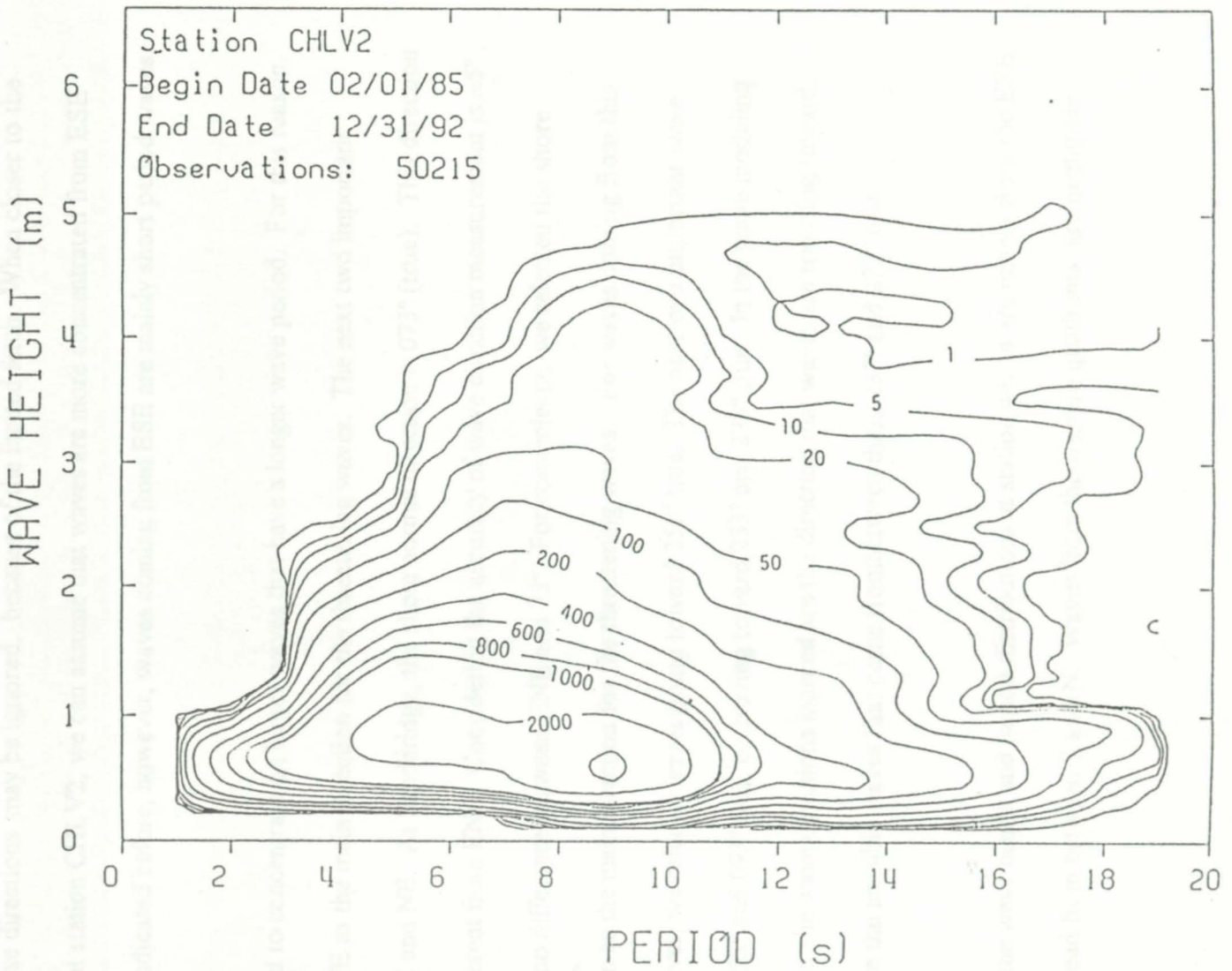

Figure 2. Joint Distribution of significant wave height and peak energy period at station CHLV2. contours number of occurrences.

Sandbridge Shoal is more than 10 m and the shoal's influence to short period waves is minimal, waves from these directions may be ignored. because of the limited fetch. When closer to the Virginia coast at station CHLV2, we can assume that waves are more concentrated from ESE direction. As indicated before, however, waves coming from ESE are mainly short period waves.

We need to concentrate on larger waves that have a longer wave period. For this reason, we selected ENE as the main direction for the threatening waves. The next two important directions are E and NE. At Sandbridge, the shore normal direction is 073° (true). This direction is only 5.5° different from ENE. Considering the accuracy of wave direction measurement is ±5° , there is almost no difference between ENE and 73°. For convenience, we selected the shore normal direction as the main direction for the threatening waves. For waves coming from this direction, however, we refer to waves going toward 253° true. The next two important wave directions are 053° and 093° true, or moving toward 233° and 273° true. In the wave modeling study given next, the wave directions marked are the direction that waves are traveling toward. We will examine the possible waves that come frombetween these 233° and 273° true.

Notice that the wave height and period distributions at station 44014 are mainly from the ESE with a large spread from between S and N. Waves from the western quadrants are negligible

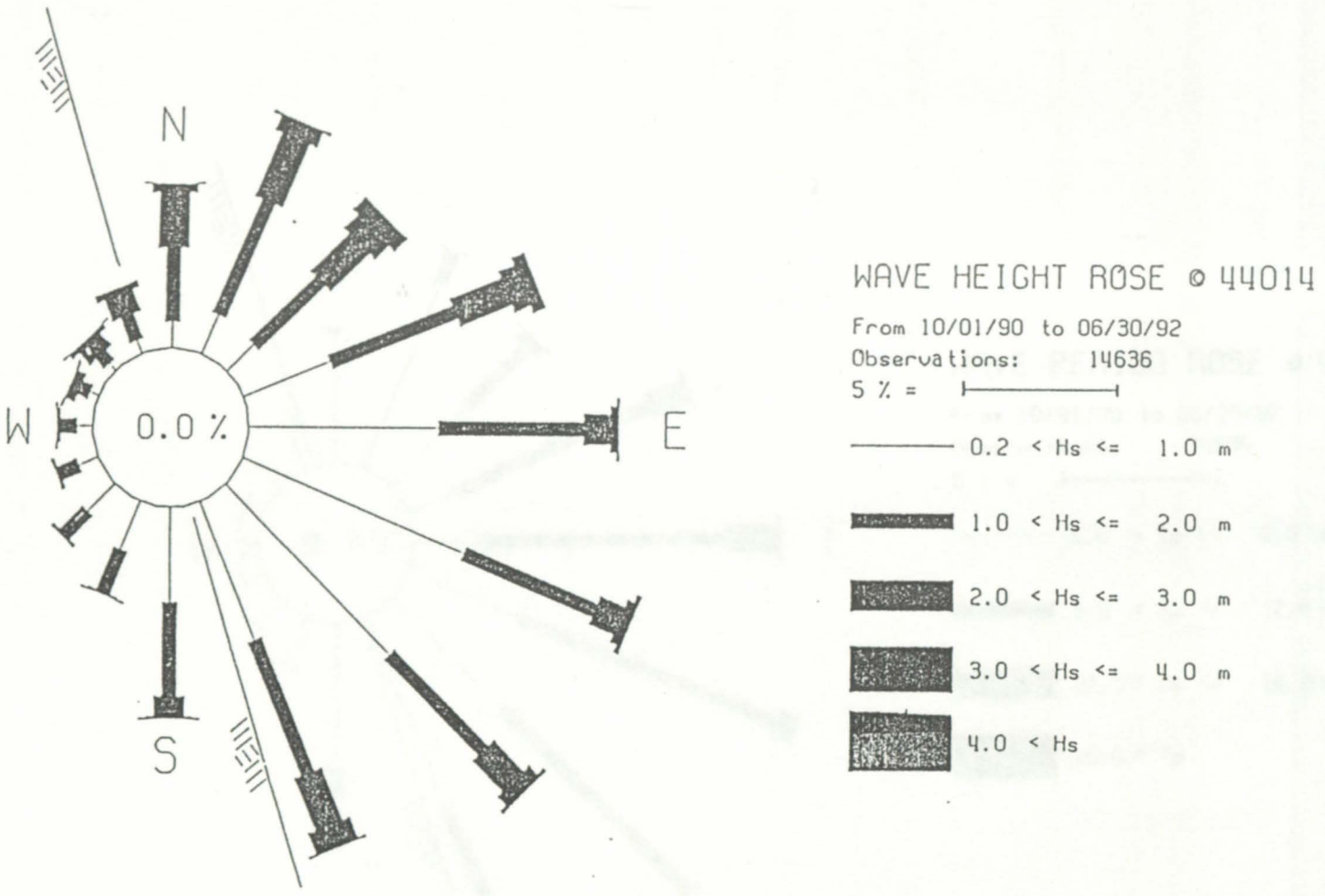

Figure 3. Wave height rose from Station 44014. The scale of occurrence is plotted in the legend.

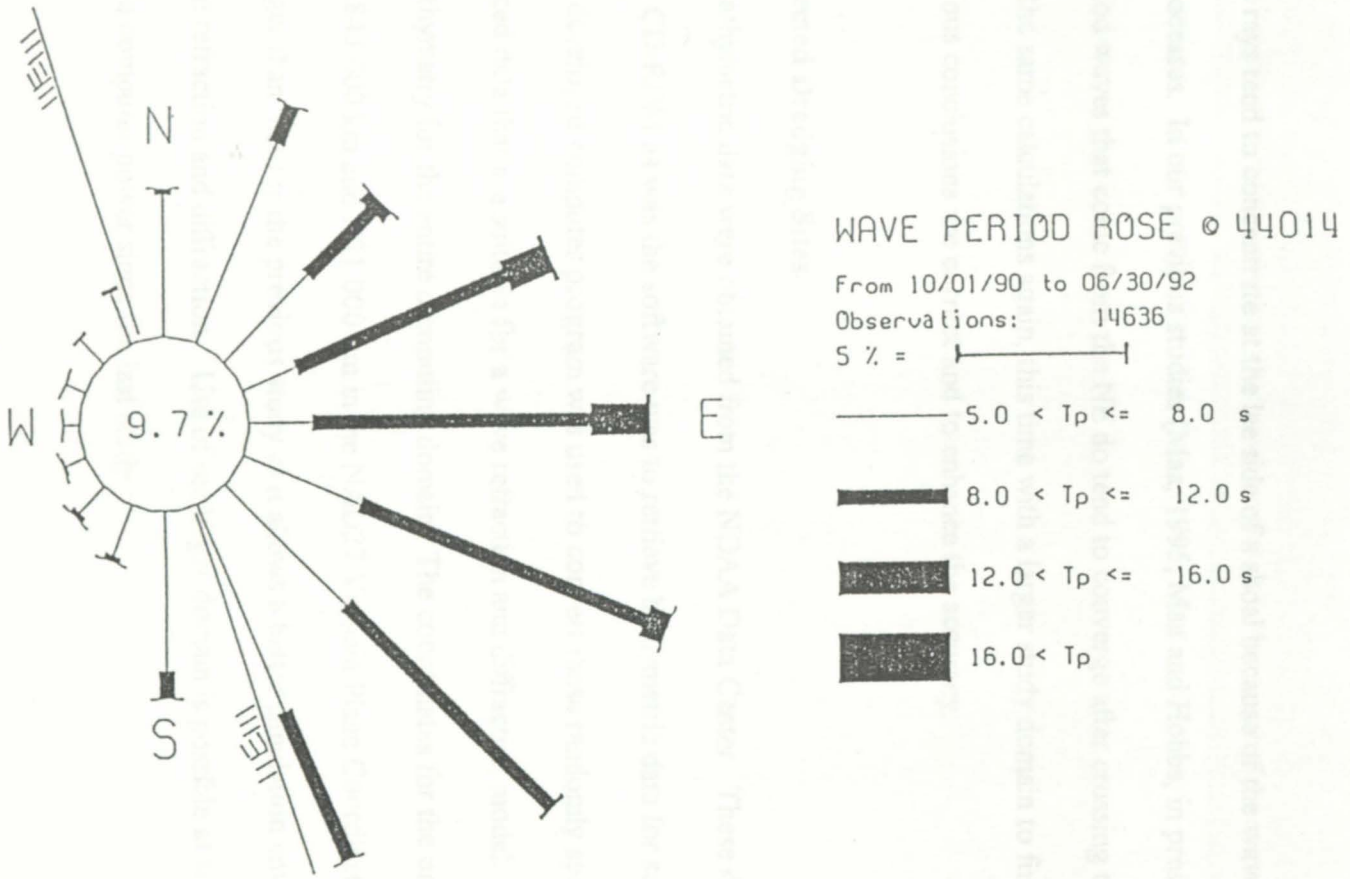

Figure 4. Wave period rose from Station 44014. The scale of 5% occurrence is plotted in the legend.

BATHYMETRY AND DREDGING SITES

Wave rays tend to concentrate at the lee side of a shoal because of the wave refraction and diffraction processes. In our previous studies (Maa, 1995; Maa and Hobbs, in press), we showed that long period waves that come from the NE do tend to converge after crossing the shoal. We will perform the same calculations again, this time with a larger study domain to further ensure that the previous conclusions are correct and to enhance the accuracy.

Original Selected Dredging Sites

The bathymetric data were obtained from the NOAA Data Center. These data were distributed in CD-ROM as was the software was to retrieve bathymetric data for selected areas. A previously developed computer program was used to convert these randomly spaced data into regularly spaced data that are suitable for a wave refraction and diffraction model. Figure 5 shows the bathymetry for the entire computing domain. The coordinates for the origin of this domain are E843.000 km and N31.000 km in the NAD27 Virginia Plane Coordinate system. This domain is larger than that for the previous study as it allows a better simulation environment in the study of wave refraction and diffraction. Use of the larger domain is possible at this time because of advances in computer power since the last study.

The size of each cell in the grid is 30 m in the X direction and 60 m in the Y direction. The small subarea enclosed by the dashed line in Figure 5 is replotted in Figure 6 to show the details of the water depth contours at the vicinity of Sandbridge Shoal. In Figure 6a, the two newly established dredging areas are also displayed: one triangle and one quadrilateral separated

by an area that is closed to dredging. The 1927 Virginia Plane State Coordinates for these corners of the two proposed dredging areas are given in Table 3. The selection of the two dredging areas was rather arbitrary and only based on the need for beach-quality sand during the next 10 years or so. The two suggested dredging areas will yield a total of 1.3×10^7 m^3 of sand if the dredging depth is a uniform 3 m within the domain.

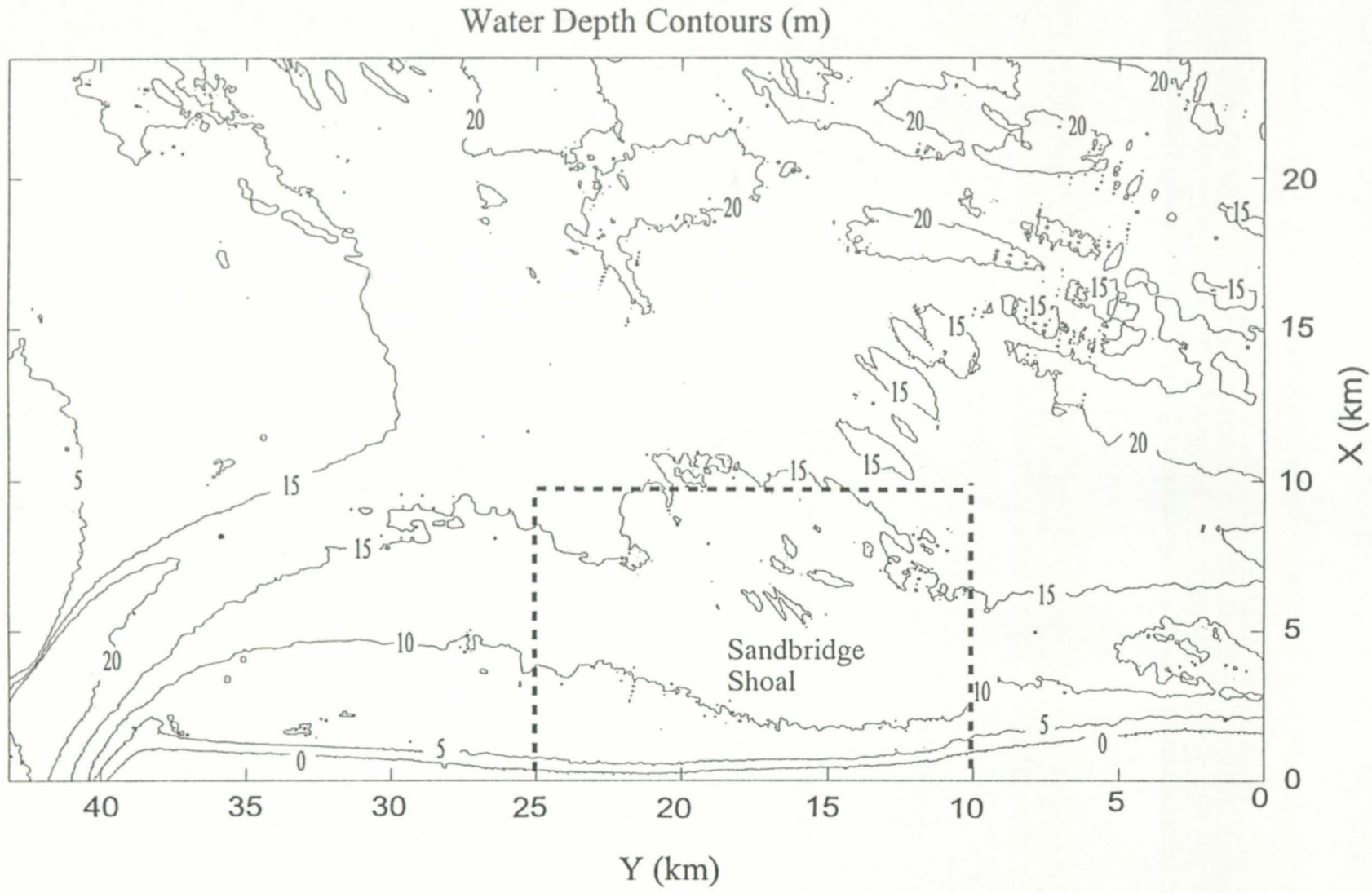

Figure 5. Water depth contours (m) for the entire study domain. More detail for the area within the dashed box are given in figure 6. Sandbridge Shoal, the target area, is shown inside the dashed lines.

Figure 6. Bathymetric details at Sandbridge Shoal. (a) The original, planned borrow sites. (b) Modified borrow sites.

Table 3

Coordinates for the Originally Selected Dredging Sites

	Site A	Site B
Area	2.1 x 10^6 m^2	2.3 x 10^6 m^2
Volume	6.3 x 10^6 m^3	6.9 x 10^6 m^3
Corner Coordinates (VA Plane Coordinate System, NAD27)		
E (m)	843,256.75	843,109.55
N (m)	47,538.35	50,722.82
E (m)	843,256.75	844,816.45
N (m)	49,144.00	51,999.90
E (m)	845,039.00	844,877.42
N (m)	48,314.96	49,457.93
E (m)	845,039.00	
N (m)	47,537.73	

Modification of Dredging Sites

While examining the proposed dredging areas, we found that some portions of the areas are already quite deep. This does not match with the idea of "removing the shoal." For this reason, we slightly changed the modeled areas that could be dredged for sand. The principle for changing the dredging area is that dredging so thatshould be carried out at the place that water depth is shallow. The new proposed dredging area is shown in Figure 6b and marked as borrow sites A and B. The possible dredging volume and coordinates for the corners are given in Table 4. Notice that after the completion of dredging at the two sites, a new shoal is created (shadow area in the middle of Figure 7) which may have an unwanted influence on wave transformation. For

Table 4

Size and coordinates for the Modified Borrow sites

Item	Borrow Site A	Borrow Site B	Borrow Site C
Area	2.3×10^6 m^2	4.5×10^6 m^2	3.5×10^6 m^2
Sand Resource	6.8×10^6 m^3	13.4×10^6 m^3	10.5×10^6 m^3
Dredging Phase	1	2	3
Corner Coordinates	(Virginia Plane Coordinate System, NAD27, m)		
1	842499.92256 49122.65848	844328.77496 52655.21562	842499.92256 49122.65848
2	844473.85805 48498.44423	845642.19101 51444.88319	844473.85805 48498.44423
3	844473.85530 46509.97286	844720.44911 49601.18703	844720.44911 49601.18703
4	843268.94961 46509.97110	842717.86320 51385.74916	842717.86320 51385.74916

this reason, we decided to examine what would happen if dredging were permitted at the remaining area of Sandbridge Shoal, *i.e.*, dredging at the area between borrow site A and B, and hereafter named borrow Site C. Currently dredging is not allowed at Site C. If the model results indicate that leaving Site C untouched is unfavorable, the prohibition on dredging in the area should be revisited.

Based on the above statements, we considered three phases: Phase 1: complete dredging of borrow site A; Phase 2: complete dredging of borrow site B; and Phase 3, complete dredging of borrow site C. The maximum amount of beach-quality sand in the three sites is about 3.1×10^8 m^3. Figure 8 depicts the water depth contours at the completion of each phase.

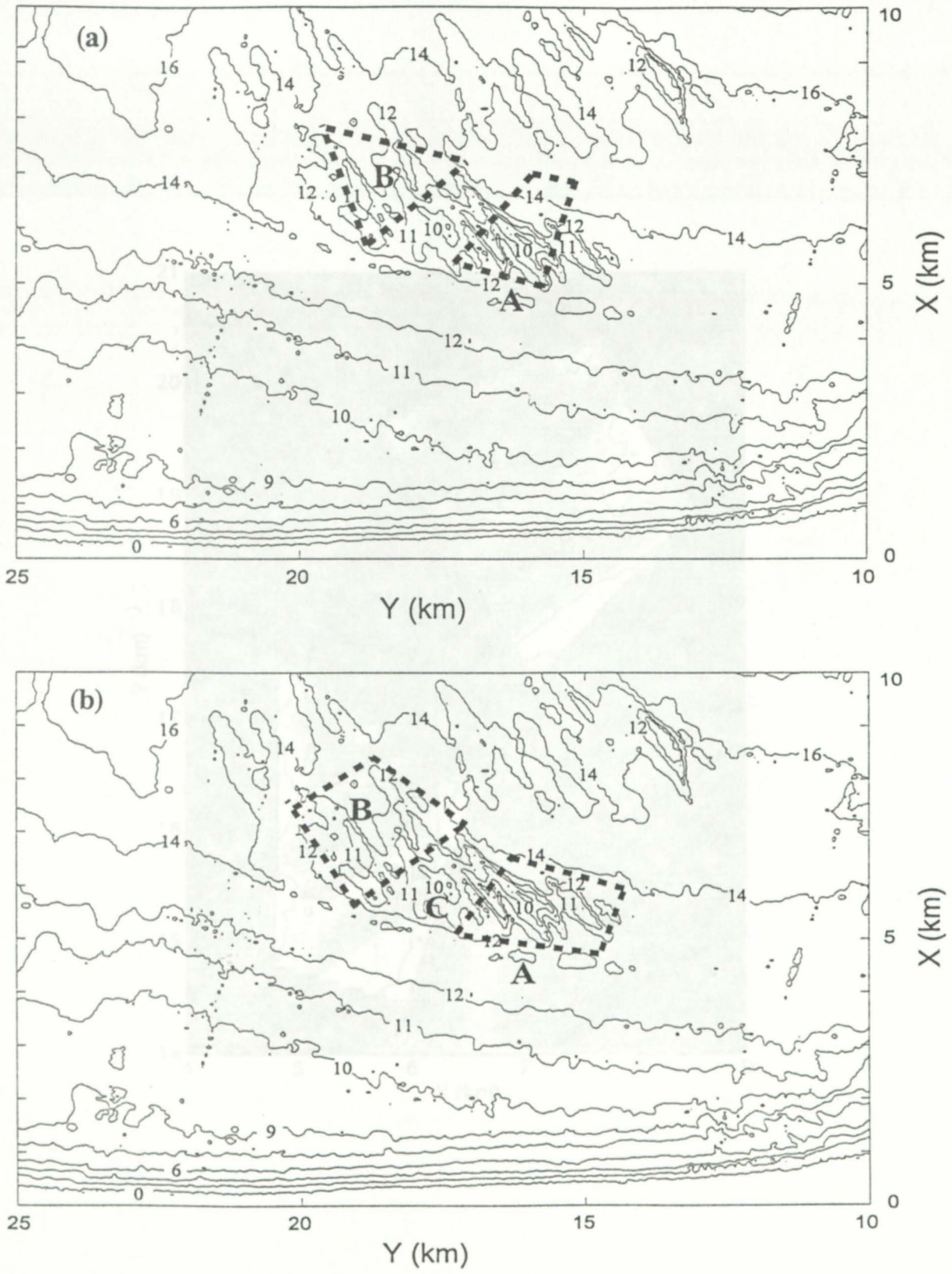

Figure 6. Bathymetric detail at Sandbridge Shoal. a) The originally planned borrow sites. b) modified borrow sites.

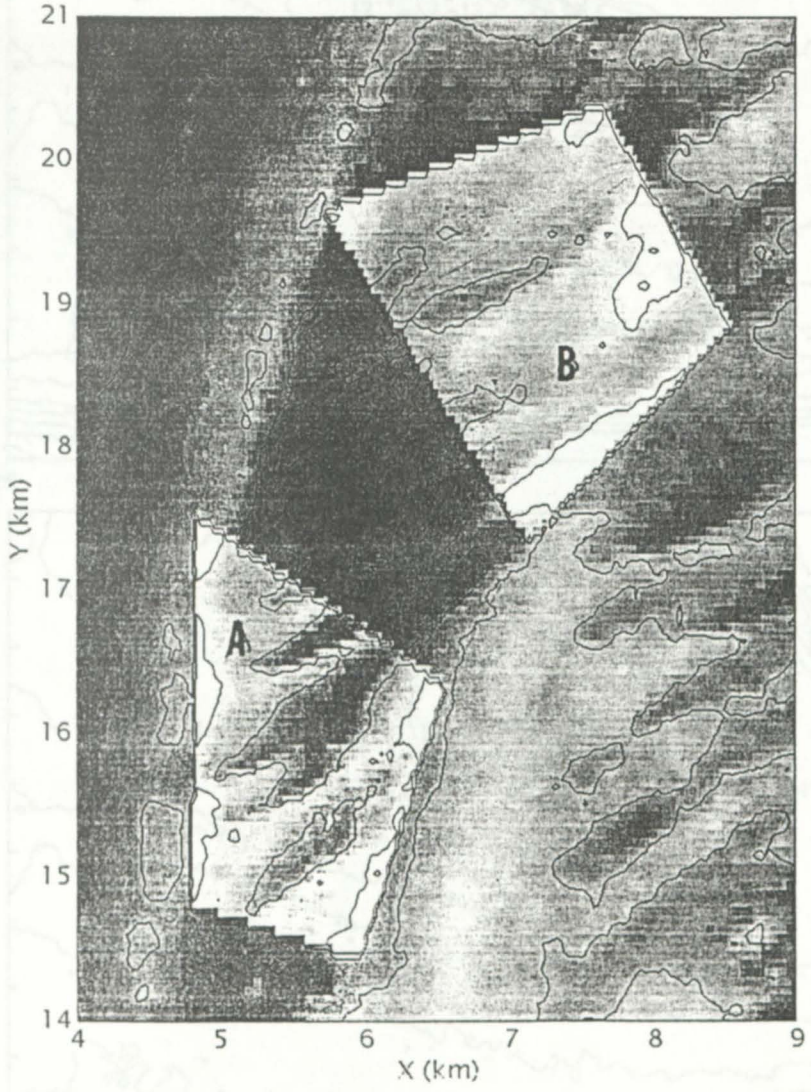

Figure 7. The area between quadrilaterals A and B is the shoal that would be left following dredging of A and B.

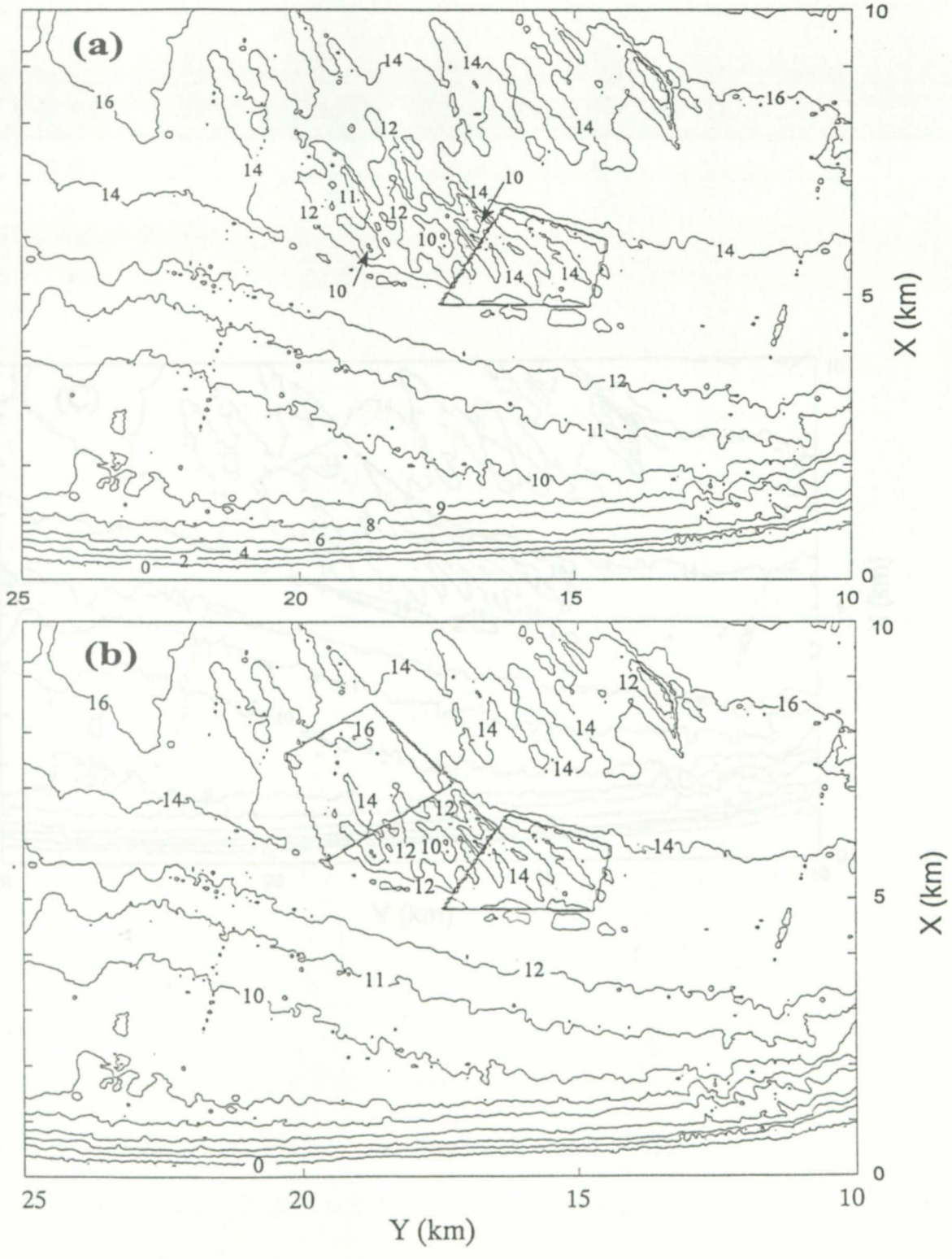

Figure 8. Bathymetric contours after the completion of dredging a) Phase 1, b) Phase 2.

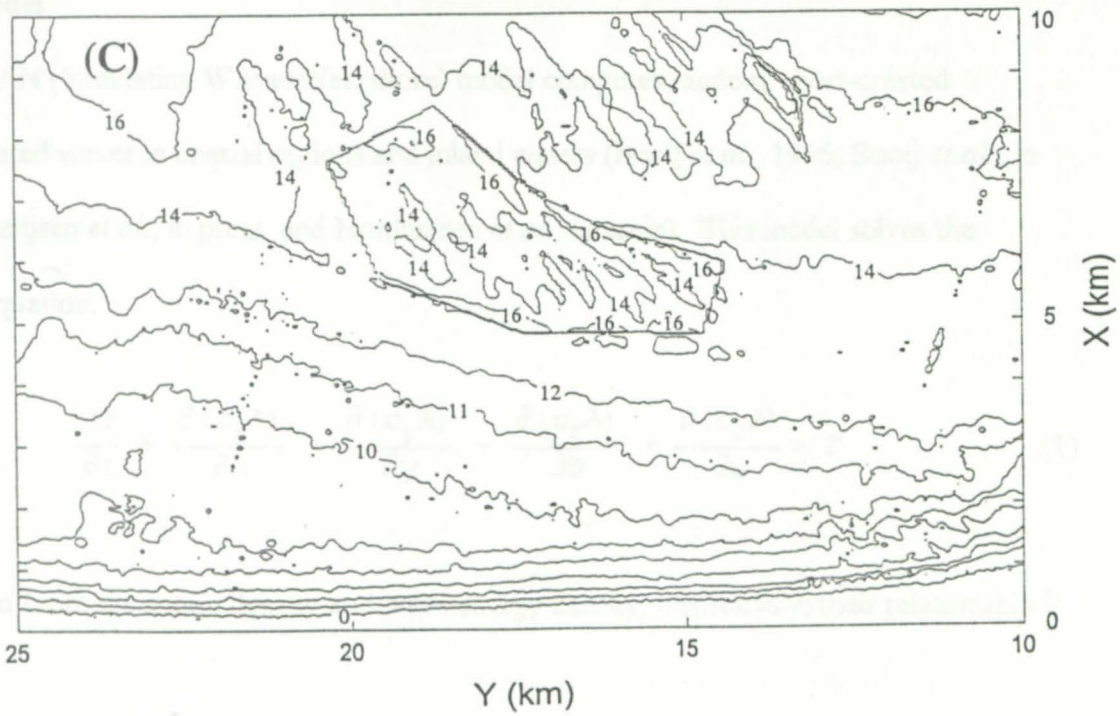

Figure 8c.. Bathymetric contours after the completion of dredging Phase 3.

WAVE TRANSFORMATION MODELS

There are many numerical models for simulating wave transformation. Each has its own strengths and weaknesses. The following are brief descriptions of each of the available models; the key features are given in Table 5.

SWAN Model

SWAN (Simulating WAves Nearshore) model computes random, short-crested wind-generated waves in coastal regions and inland waters (Booij *et al.*, 1996; Booij *et al.*, in press; Holthuijsen *et al.*, in press and Holthuijsen *et al.*, in press). This model solves the following equation:

$$\frac{\partial A}{\partial t} + \frac{\partial (c_x A)}{\partial x} + \frac{\partial (c_y A)}{\partial y} + \frac{\partial (c_\theta A)}{\partial \theta} + \frac{\partial (c_\omega A)}{\partial \omega} = T \qquad (1)$$

where A and E are the action density and wave energy density, respectively; their relationship is given next.

$$A(x, y, \theta, \omega) = E(x, y, \theta, \omega) / (\omega - k \cdot V) \qquad (2)$$

Where x and y are horizontal plane coordinates, θ is wave direction, ω is wave frequency, k is wave number vector, and V is current velocity. The right hand term, T, includes several energy sources (*e.g.*, wind energy, wave-wave interaction) and sinks (*e.g.*, bottom friction, white capping, wave breaking). Although this equation is a first order partial differential equation, there are four variables, thus, solving the equation is very time consuming. Also, the difficult part of

solving this equation is the accurate inclusion of the all the source and sink functions.

The current SWAN model is Cycle 2 with version 30.62. It accounts for the following physics: wave propagation in time and space, shoaling, refraction due to current and depth, frequency shifting due to currents and non-stationary depth, wave generation by wind, three- and four-wave interactions, white capping, bottom friction, and depth-induced breaking. SWAN computations can be made on regular and curvilinear grids in a Cartesian coordinate system. Because no diffraction is considered, the grid size can be much larger when compared with wave length (L/2). Even with a relatively large grid size, the computing time is formidably long because of the complexity of this wave spectrum transformation equation (Eq. 1). For this reason, we can not afford to use it at this time.

RDE Model

The RDE model solves the extended mild slope equation, Eq. N (Massel 1995) using the Gaussian elimination method with partial pivoting and a special book-keeping procedure for simulating water-wave refraction, diffraction, shoaling, reflection, and resonance (Maa and Hwung, in press). This finite difference model only requires sufficient hard disk space to handle realistic applications using small computers. Because of the finite difference method and the direct approach to solving the governing equation, this model is simple to maintain, and more importantly, is easy to upgrade with other processes, *e.g.*, bottom friction, tidal current influence, and spectrum waves, in the future.

$$\nabla^2\phi + \frac{e_0}{h}\nabla h\cdot\nabla\phi + k^2[1 + e_1\nabla h\cdot\nabla h + \frac{e_2}{k_0}\nabla^2 h]\phi = 0 \qquad (3)$$

where

$$e_0 = \frac{kh}{\tanh kh + kh(1-\tanh^2 kh)}(1 - 3\tanh^2 kh + \frac{2tanhkh}{\tanh kh + kh(1-\tanh^2 kh)}) \quad (4)$$

$$e_1 = \frac{1}{n\tanh kh} \cdot \frac{1}{24(2kh + \sinh 2kh)^2 \cosh^3 kh} \cdot$$

$$\{ kh[12+16(kh)^2] \cosh kh + 6kh[\cosh 3kh + \cosh 5kh] +$$

$$[12+84(kh)^2]\sinh kh + 3[1-4(kh)^2]\sinh 3kh - 9\sinh 5kh \} \quad (5)$$

$$e_2 = \frac{1}{n}[\frac{-4kh \cosh kh + \sinh kh + (kh)^2\sinh kh + \sinh 3kh}{8(2kh + \sinh 2kh)\cosh^3 kh} - \frac{kh}{2}\frac{\tanh kh}{\cosh^2 kh}] \quad (6)$$

$$n = \frac{1}{2}\left[1 + \frac{2kh}{\sinh(2kh)}\right] \quad (7)$$

ϕ is the velocity potential function for a simple harmonic wave flow, $k_o = 4\pi^2/gT^2$ is the deep water wave number, T is the wave period, g is gravitational acceleration, $k = 2\pi/L$ is the local wave number, L is the local wave length, h is the water depth, ∇h is the bottom slope, $(\nabla h)^2$ and $\nabla^2 h$ are bottom slope square and bottom curvature, respectively.

The major area of application for this model, however, is for harbor planning because wave reflection, resonance, and strong diffraction are important features for harbor planning purposes. This model is not recommended for the current study because: (1) wave reflection and resonance are not important along open coasts; (2) only weak diffraction is needed for open coasts; and (3) the small grid size (less than one-tenth of wave length) required causes low computing efficiency.

Nevertheless, the RDE model solves the original elliptic equation in a more rigorous manner, the output from the RDE model will be used as a base with which to compare the results obtained from the next two model results: REF/DIF-1 and RCPWAVE.

The typical elliptic shoal problem given by Berkhoff (1972) Berkhoff *et al.* (1982) was selected to examine the performance of the different models. A relatively uneven wave height for the area before the shoal is obvious in the normalized wave height contours plot generated by using the RDE model (Fig. 9). This relatively uneven wave height may be caused by small reflective waves generated from the slope bottom. Since the complex velocity potential function can carry wave phase information, the wave phase information can be used to generate a plot of wave crests (Fig. 10). Using the phase information, wave vectors also can be plotted (Fig. 11). Because of the small grid size required for the RDE model, only one from every six vectors was plotted for obtaining a clear picture. This diagram clearly shows the convergence of waves after the shoal and the wave trajectories (Fig. 12) may cross each other after the shoal. The wave trajectory plot did not show the wave rays crossing each other directly because it uses local wave direction information, which represents the dominant wave direction, to construct the trajectories.

Because of the divergence after the convergent area, it is reasonable to assume that wave trajectories do cross each other.

Figure 9: Normalized wave height contours obtained using the REF/DIF model.

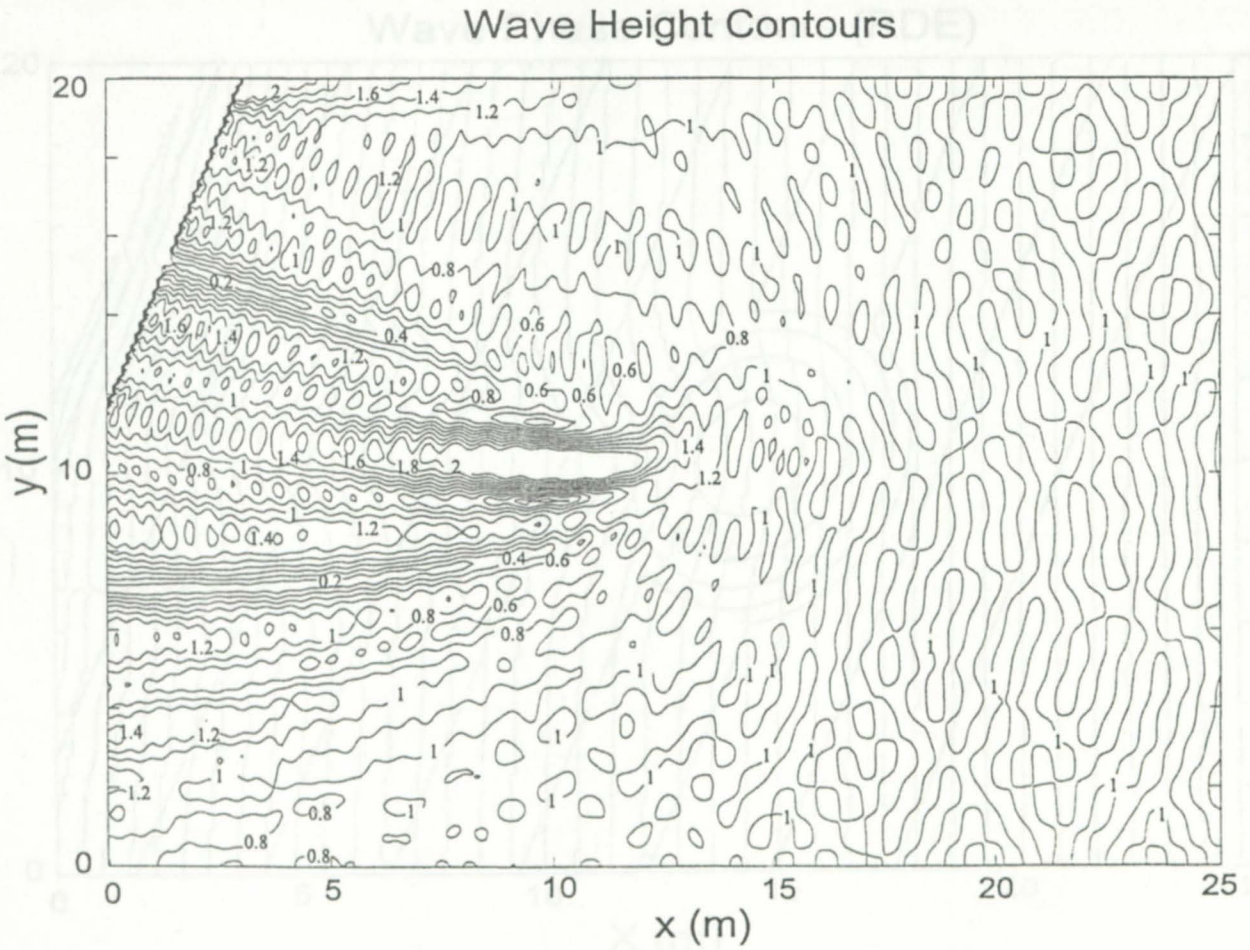

Figure 9: Normalized wave height contours obtained using the RDE model.

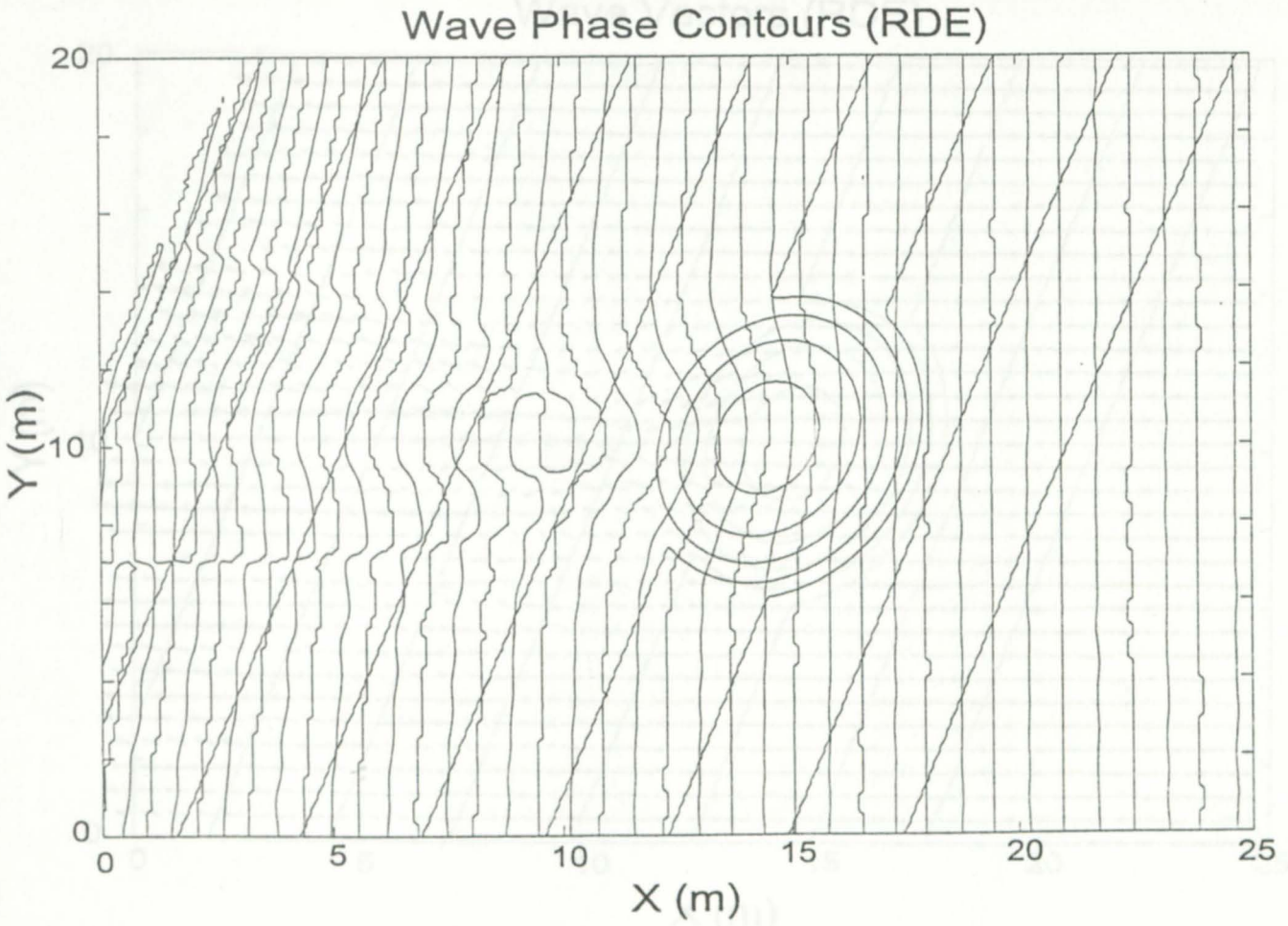

Figure 10: Calculated wave phases which represent wave crests obtained used the RDE model.

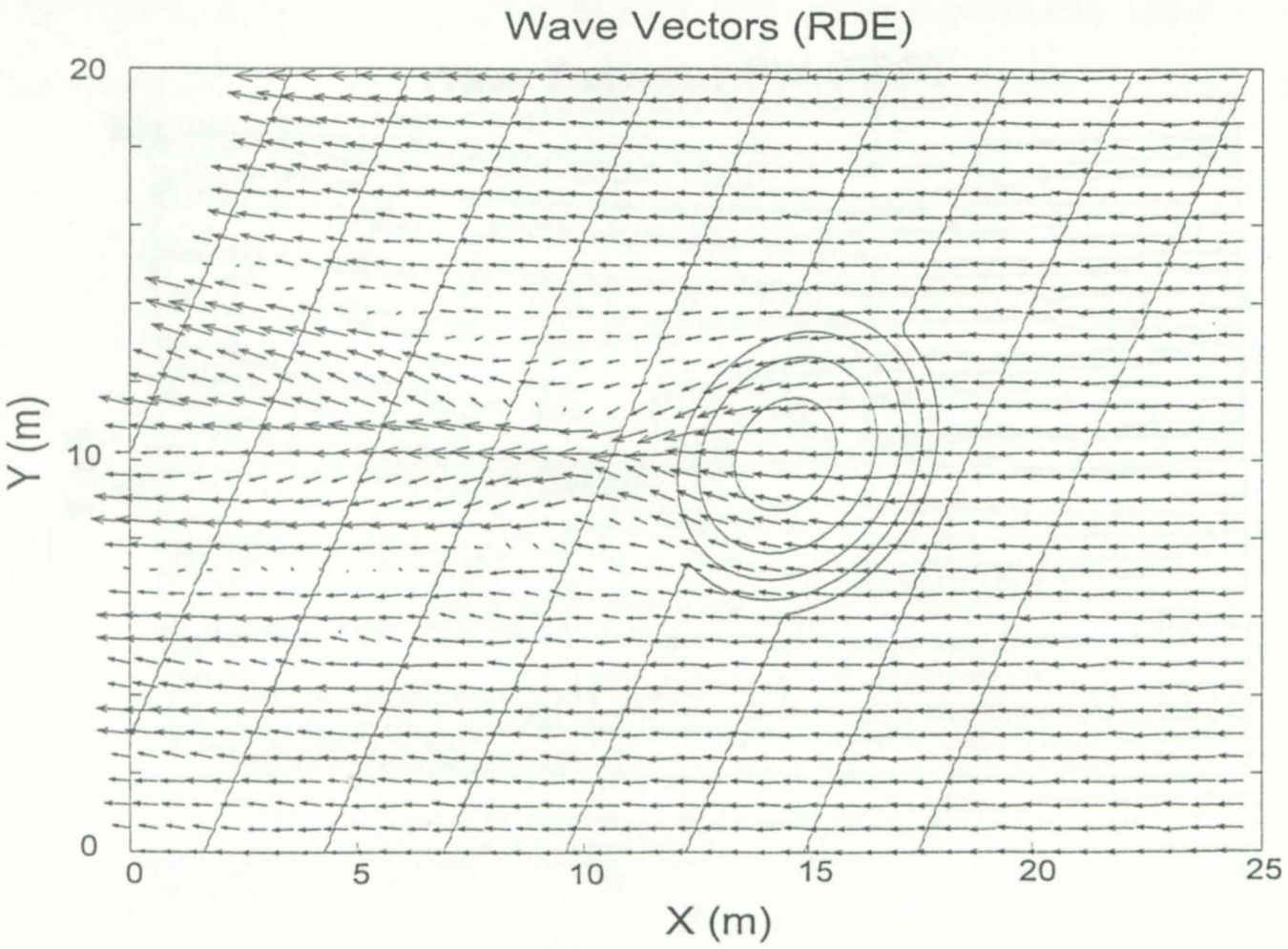

Figure 11: Wave vectors calculated with the RDE Model.

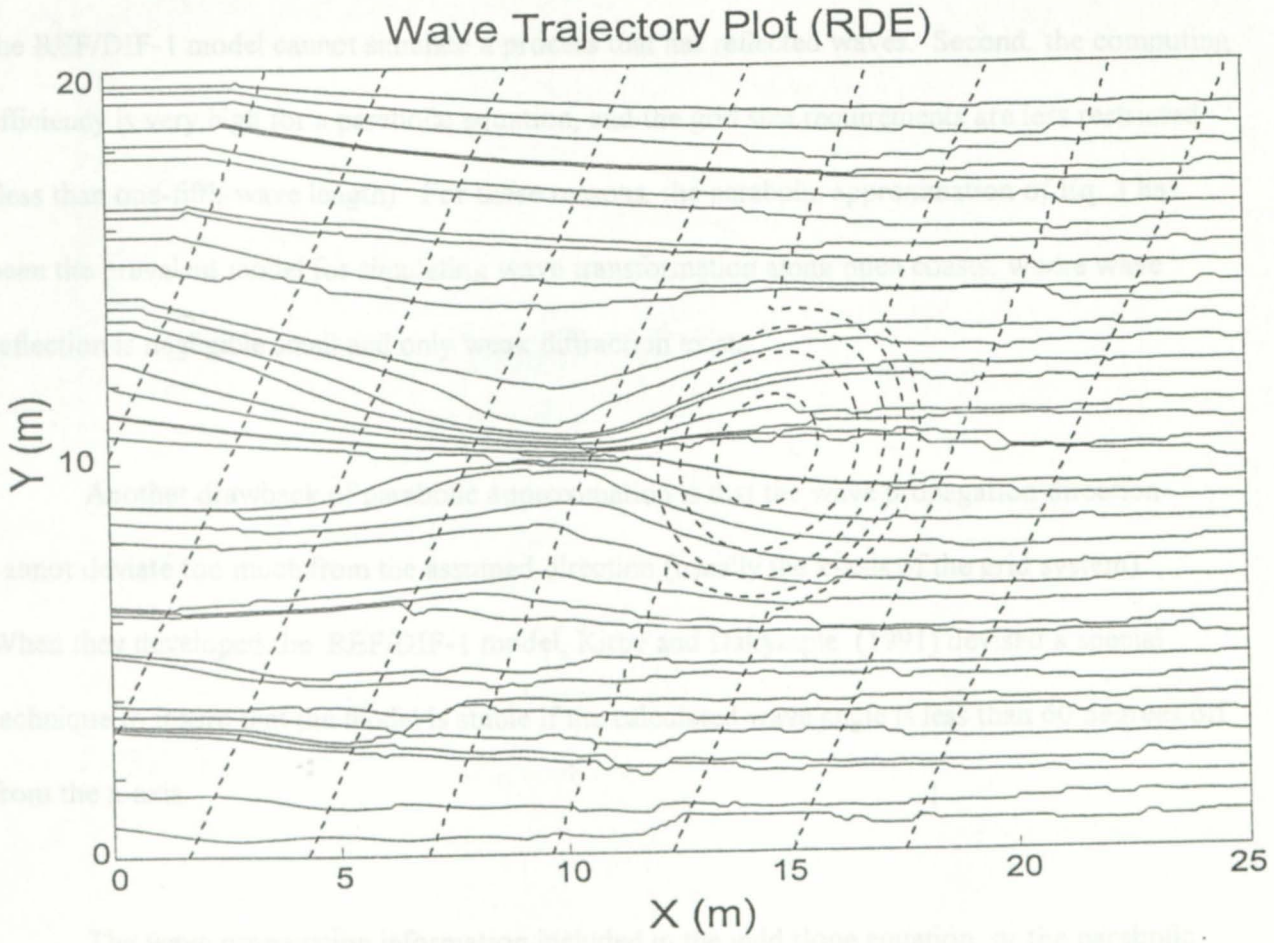

Figure 12: Wave trajectories calculated with the RDE model.

REF/DIF-1 Model

The mild slope equation given by Berkhoff (1972, Eq. 3) without the bottom slope square and bottom curvature terms) is a good approximation for wave transformation. Because the mild slope equation is an elliptic equation, it cannot be solved efficiently. Radder (1979) developed a parabolic approximation of Eq. 3 which has several advantages over the original elliptic equation. First, the down-wave boundary conditions are not needed for a parabolic equation. This implies the REF/DIF-1 model cannot simulate a process that has reflected waves. Second, the computing efficiency is very high for a parabolic equation, and the grid size requirements are less restricted (less than one-fifth-wave length). For these reasons, the parabolic approximation of Eq. 3 has been the prevalent model for simulating wave transformation along open coasts, where wave reflection is negligible small and only weak diffraction exists.

Another drawback of parabolic approximation is that the wave propagation direction cannot deviate too much from the assumed direction (usually the x-axis of the grid system). When they developed the REF/DIF-1 model, Kirby and Dalrymple (1991) devised a special technique to insure that the model is stable if the calculated wave angle is less than 60 degrees off from the x-axis.

The wave propagation information included in the mild slope equation, or the parabolic approximation, contains both the wave height and the wave phase. Figure 13 shows the calculated wave height contours (normalized with the input wave height) for the wave refraction and diffraction experiment carried out by Berkhoff *et al.* (1982) using the REF/DIF-1 model. Because there are only progressive waves in the computing domain, the wave heights are quite

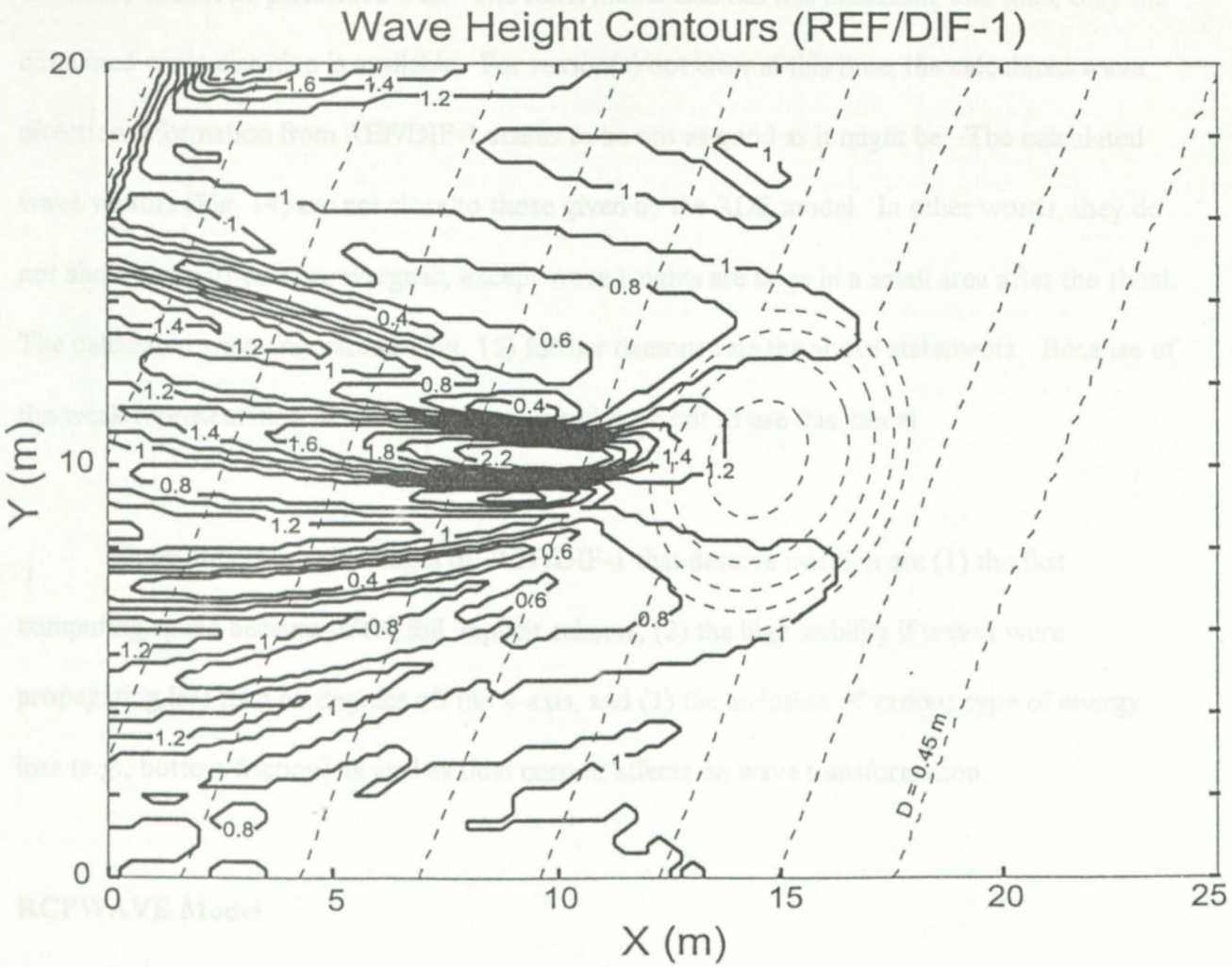

Figure 13. Normalized wave height contours obtained using the REF/DIF-1 model.

smooth and all the wave height exactly equal to 1 before the shoal.

When two waves cross each other, however, the information for two wave phases is contained in one variable. For this reason, the calculation of wave phase, and then, wave direction, cannot be performed well. The RDE model also has this limitation, and thus, only the combined wave direction is available. For reason(s) not clear at this time, the calculated wave direction information from REF/DIF-1 seems to be not as good as it might be. The calculated wave vectors (Fig. 14) are not close to those given by the RDE model. In other words, they do not show any particular convergenc, except wave heights are large in a small area after the shoal. The calculated wave trajectories (Fig. 15) further demonstrate the above statements. Because of the weak representation of wave direction, we choose not to use this model.

Three important advantages of REF/DIF-1 that deserve mention are (1) the fast computing speed because of the full implicit scheme, (2) the high stability if waves were propagating less than 60 degrees off the x-axis, and (3) the inclusion of various type of energy loss (*e.g.*, bottom friction) as well as tidal current effects on wave transformation.

RCPWAVE Model

In order to obtain clear information on wave direction for calculating longshore sediment transport, Ebersole (1985) developed the RCPWAVE model by solving the mild slope equation (Eq. 3 without the bottom curvature and bottom slope square terms) with an additional restriction (Eq. 8) which represents the irrotational condition:

$$\nabla \times \nabla S = 0 \qquad (8)$$

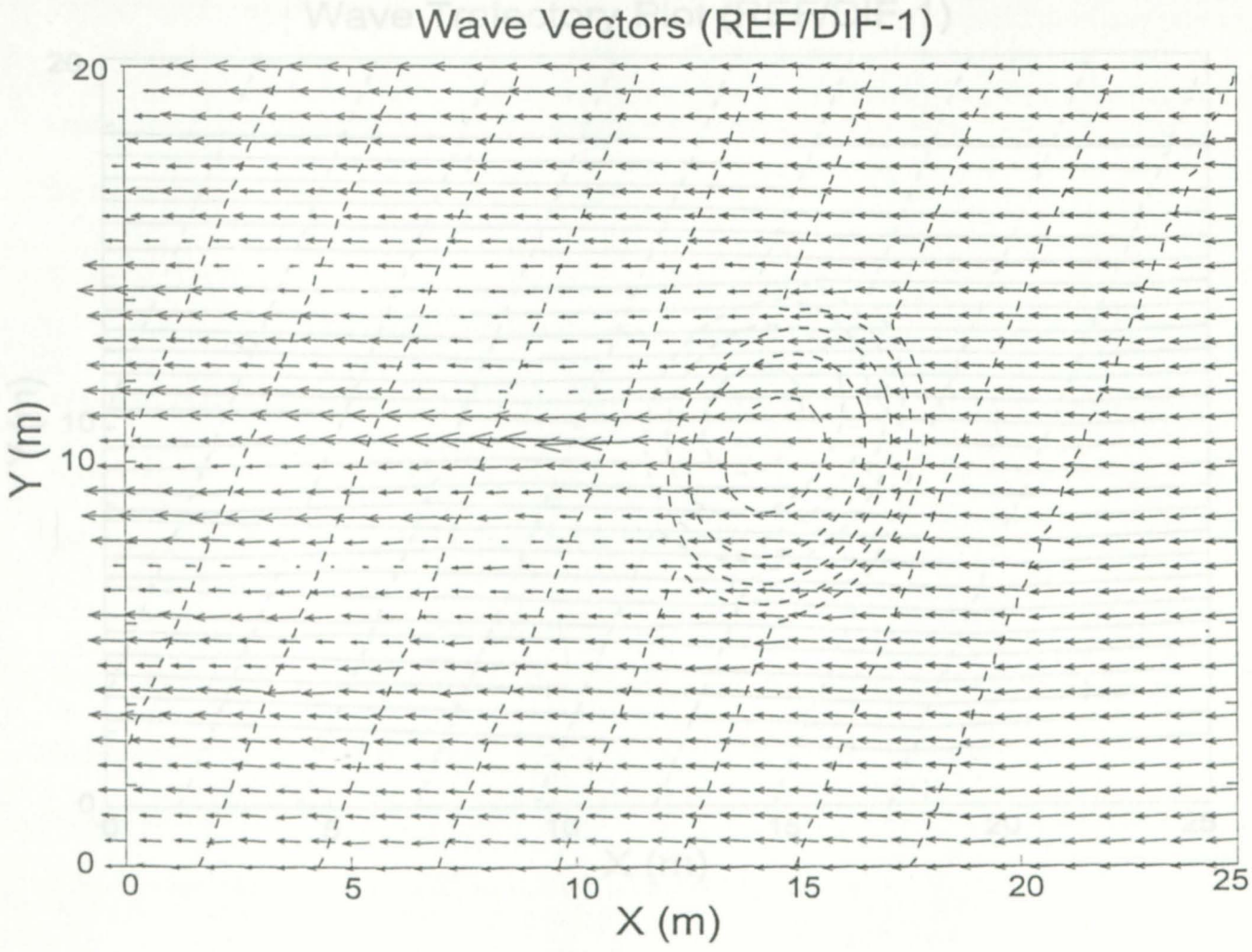

Figure 14: Wave vectors calculated RED/DIF-1.

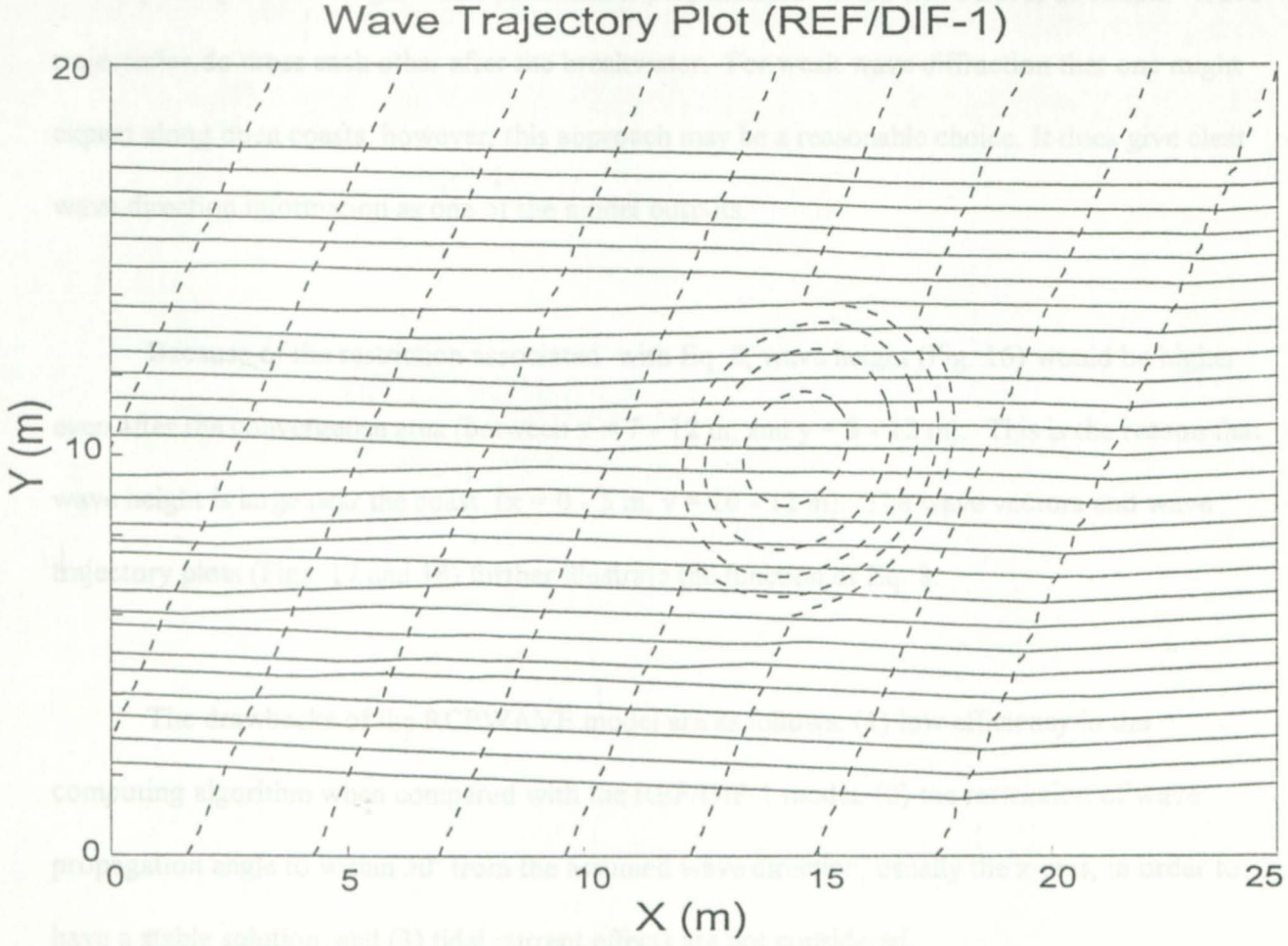

Figure 15: Wave trajectories calculated with REF/DIF-1.

where S is the phase function. This restriction further constrains that wave trajectories will not cross each other. In cases where two wave rays converge, this method insures that the wave trajectories will just get closer and closer. For strong diffraction, this criterion is not acceptable because wave trajectories do cross, for example, the case study given by Goda *et al.* (1971) for waves passing a finite length breakwater that is perpendicular to the wave travel direction. Wave trajectories do cross each other after the breakwater. For weak wave diffraction that one might expect along open coasts, however, this approach may be a reasonable choice. It does give clear wave direction information as one of the model outputs.

Because of the restriction associated with Eq. 8, wave height (Fig. 16) would be higher even after the convergence area (between x = 7 - 12 m, and y = 8 - 12 m). This is the reason that wave height is large near the coast (x = 0 - 5 m, y = 10 - 12 m). The wave vectors and wave trajectory plots (Figs. 17 and 18) further illustrate the function of Eq. 8.

The drawbacks of the RCPWAVE model are as follows: (1) low efficiency in the computing algorithm when compared with the REF/DIF-1 model, (2) the restriction of wave propagation angle to within 30° from the assumed wave direction, usually the x-axis, in order to have a stable solution, and (3) tidal current effects are not considered.

In summary, the last two models that are feasible for applying to large open coasts each have drawbacks and advantages. The RCPWAVE model may overestimate the breaking wave height, and the REF/DIF-1 may underestimate the breaking wave height. For wave direction information, RCPWAVE is better than REF/DIF-1. Since overestimation is on the safe

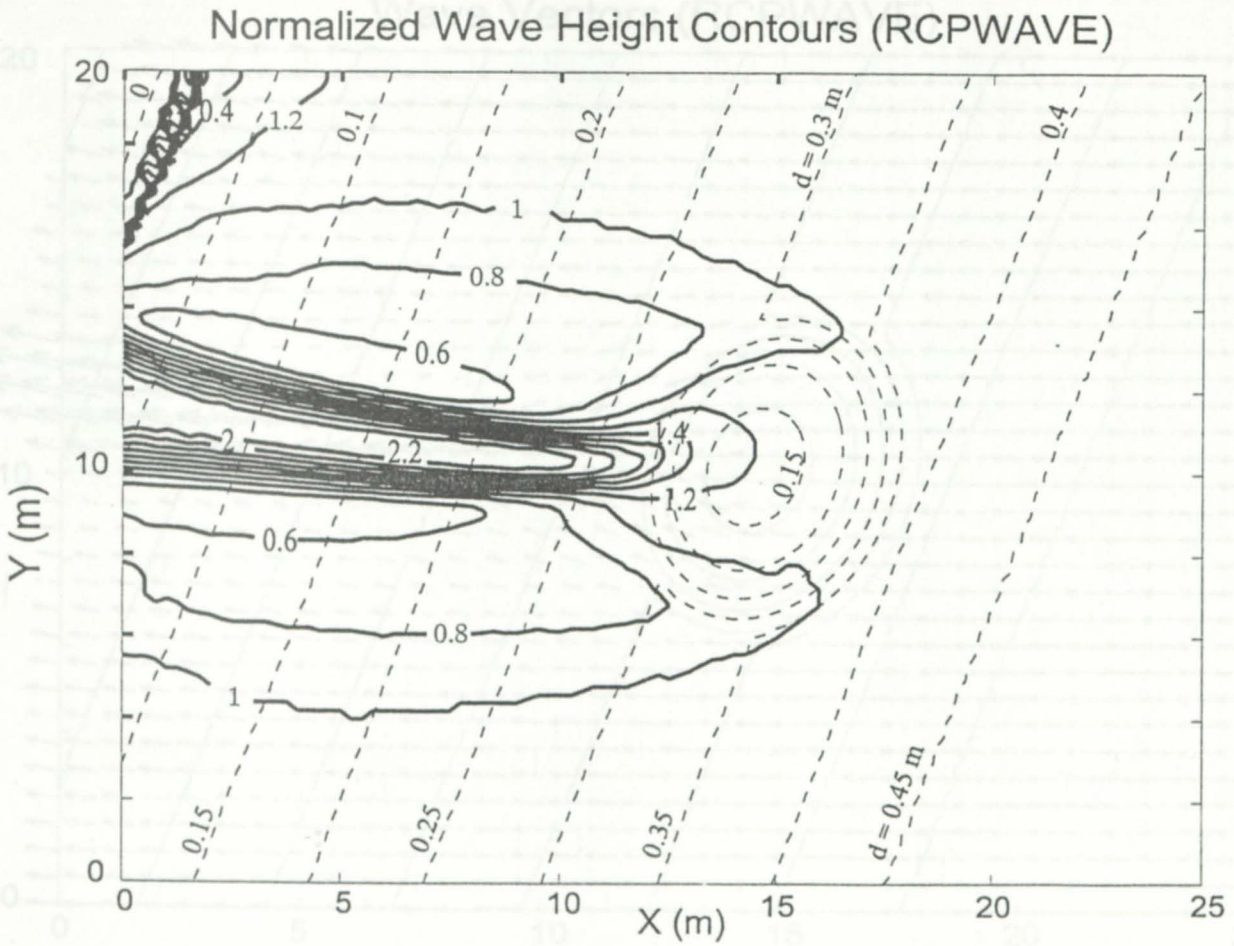

Figure 16: Normalized wave height contours obtained with RCPWAVE.

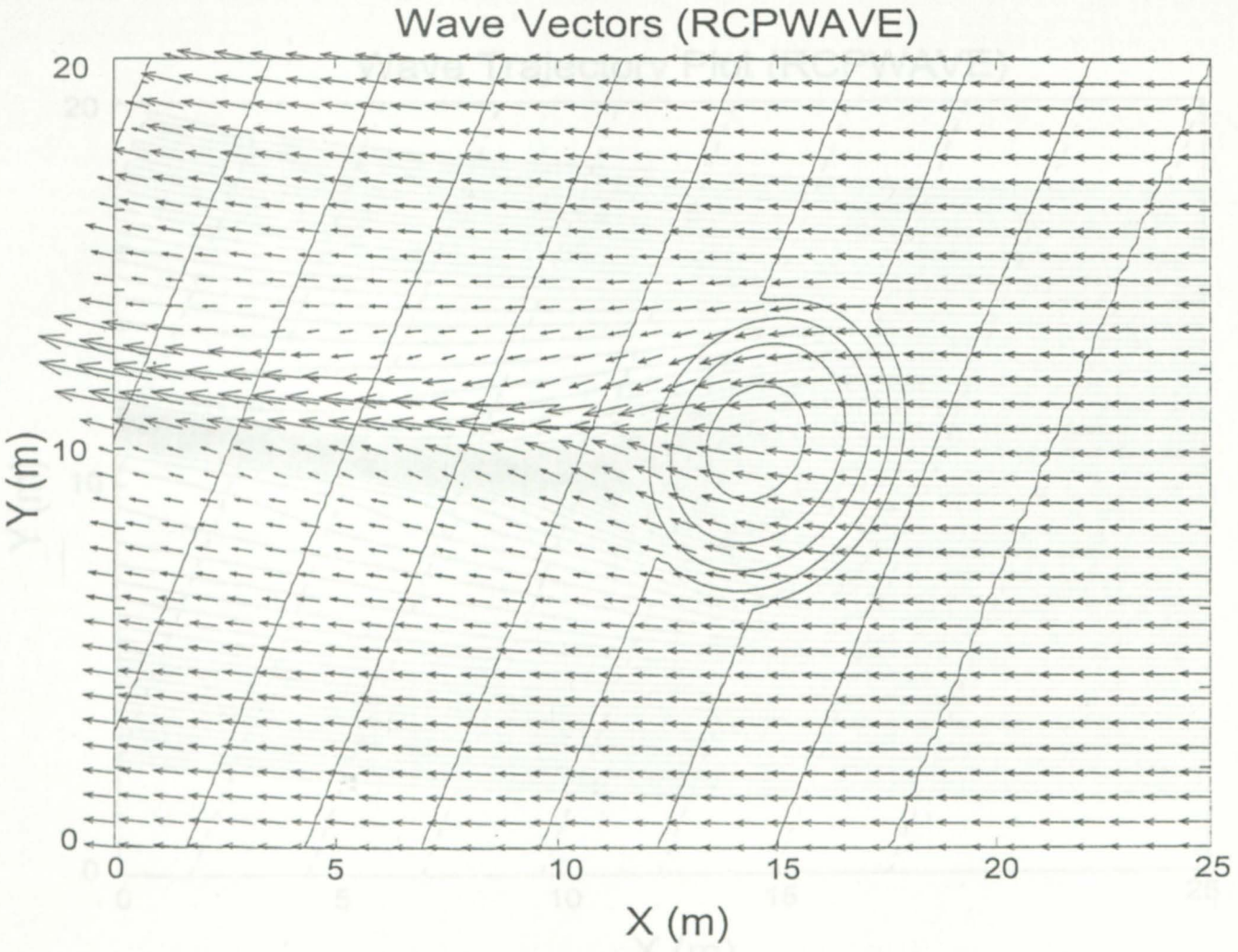

Figure 17: Wave vectors calculated with RCPWAVE.

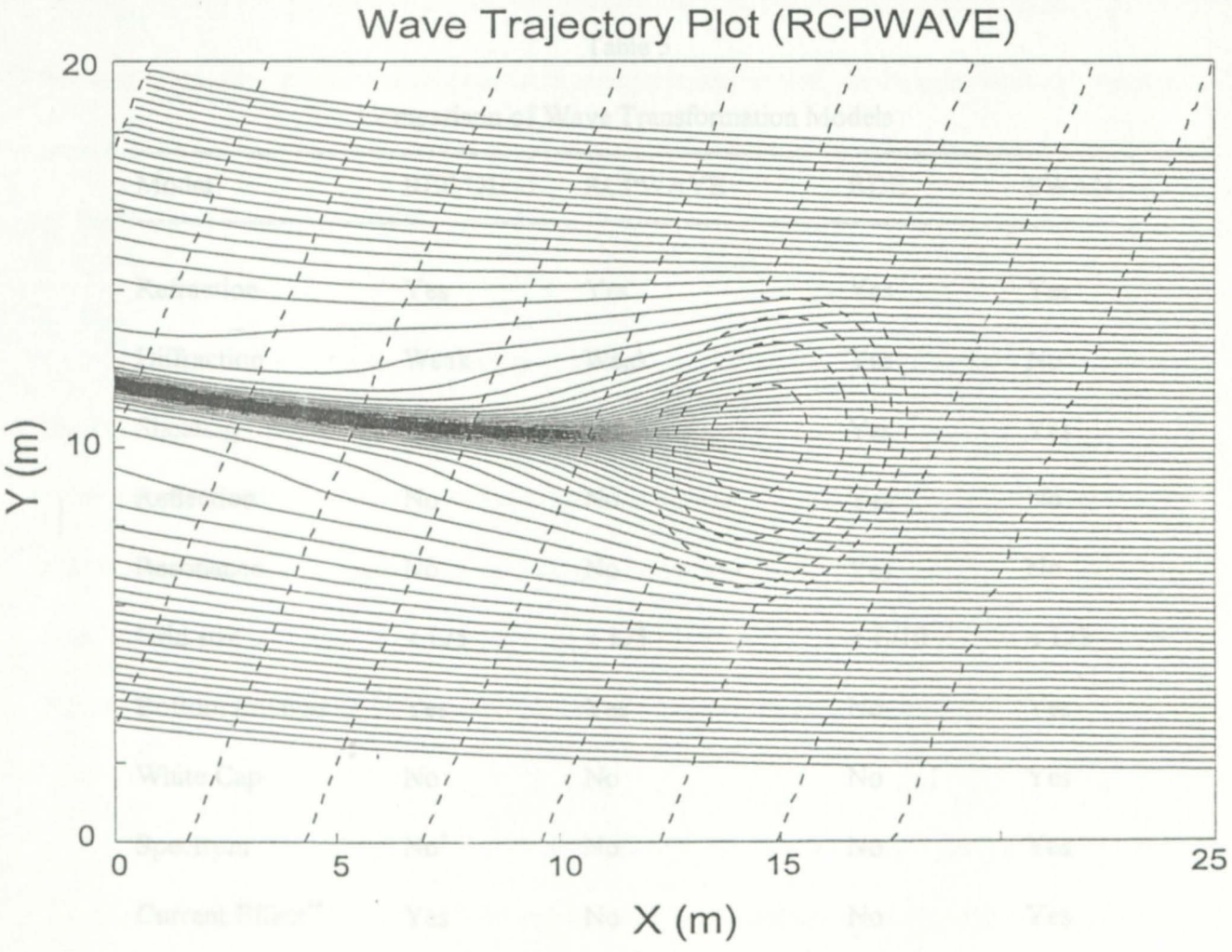

Figure 18: Wave trajectories calculated with RCPWAVE.

side for estimating longshore sediment transport, we prefer the RCPWAVE model. Our objective is to employ a model that best meets our objectives for examining the possible difference caused by the accumulated dredging at Sandbridge Shoal. Given this summary and that the wave breaking angles needed for next phase study are available from the RCPWAVE, we chose the RCPWAVE model in this study

Table 5

Comparison of Wave Transformation Models

Model	REF/DIF-1	RCPWAVE	RDE	SWAN
Refraction	Yes	Yes	Yes	Yes
Diffraction	Weak	Weak	Yes	No
Shoaling	Yes	Yes	Yes	Yes
Reflection	No	No	Yes	No
Resonance	No	No	Yes	No
Grid size	≤ L/5	≤ L/5	≤ L/10	≤ L/2
Bottom Friction	Yes	Yes	No	Yes
White Cap	No	No	No	Yes
Spectrum	No*	No	No	Yes
Current Effect**	Yes	No	No	Yes
Computing Speed	Excellent	Good	Fair	Fair

* Available for a late version REF/DIF-S, but wave-wave interaction is not included.

** The formulation and codes have included the influence of tidal current. A detailed tidal current fields, however, have to be obtained from other sources.

WAVE TRANSFORMATION FOR THE ORIGINAL BATHYMETRY

In our earlier study we (Maa, 1995; Maa and Hobbs, in press) demonstrated that Sandbridge Shoal would not have a calculable influence on waves with a period shorter than 9 seconds and that the change of wave conditions resulting from a small amount of dredging (on the order of 10^6 m^3) would be limited to about 5%, which cannot be classified as significant because it is within the accuracy of the wave measurement system. In the present study, we will examine the possible changes to the wave regime after substantial dredging at the shoal according to the three phases given in Table 4.

For the three wave conditions (most severe sea, severe sea, and northeaster wave), we ran the RCPWAVE model with six possible wave directions; 233°, 243°, 253°, 263°, and 273°. Again these angles are the directions that wave trains move toward. Figures 19a, b, and c show the calculated wave rays for the northeaster waves coming from 233°, 253°, and 273°, respectively. Only the section of the entire study grid from y = 10 to 30 km is presented here for a clear view. Figures 20 and 21 show similar plots for the severe sea and the most severe sea.

In general, waves tend to converge near Sandbridge for all the wave directions selected. As waves are higher in the zone of convergence, this might explain the severe beach erosion at Sandbridge. Notice that as the wave period decreases, the wave ray convergence also decreases. In other words, the longer the wave period, the more beach erosion at Sandbridge.

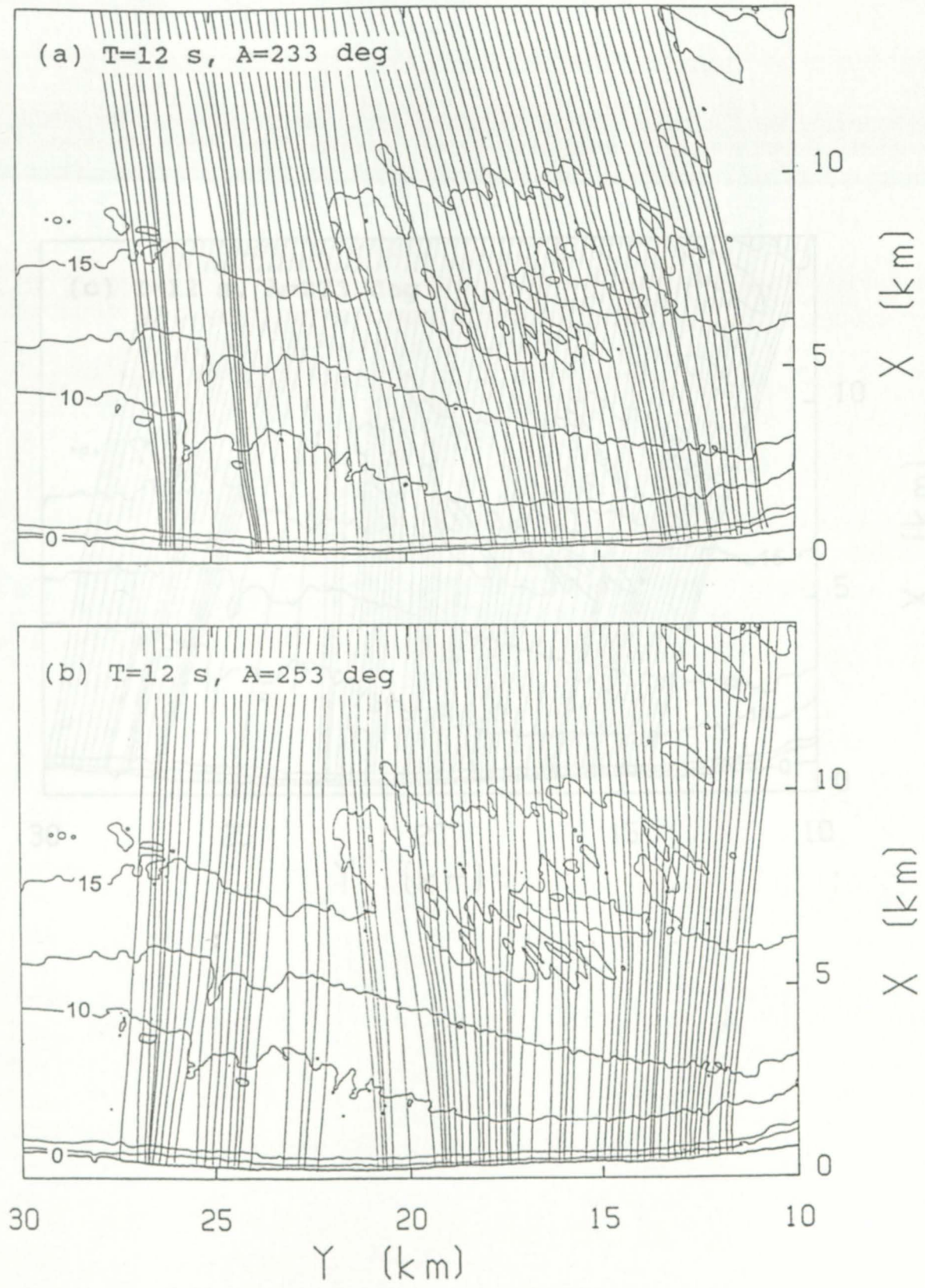

Figure 19. Calculated wave rays for the Northeaster wave (H = 1.9 m, T = 12 s) for the existing bathymetry. a) Waves approaching from the NE (233°). b) Waves approaching from the ENE (253°).

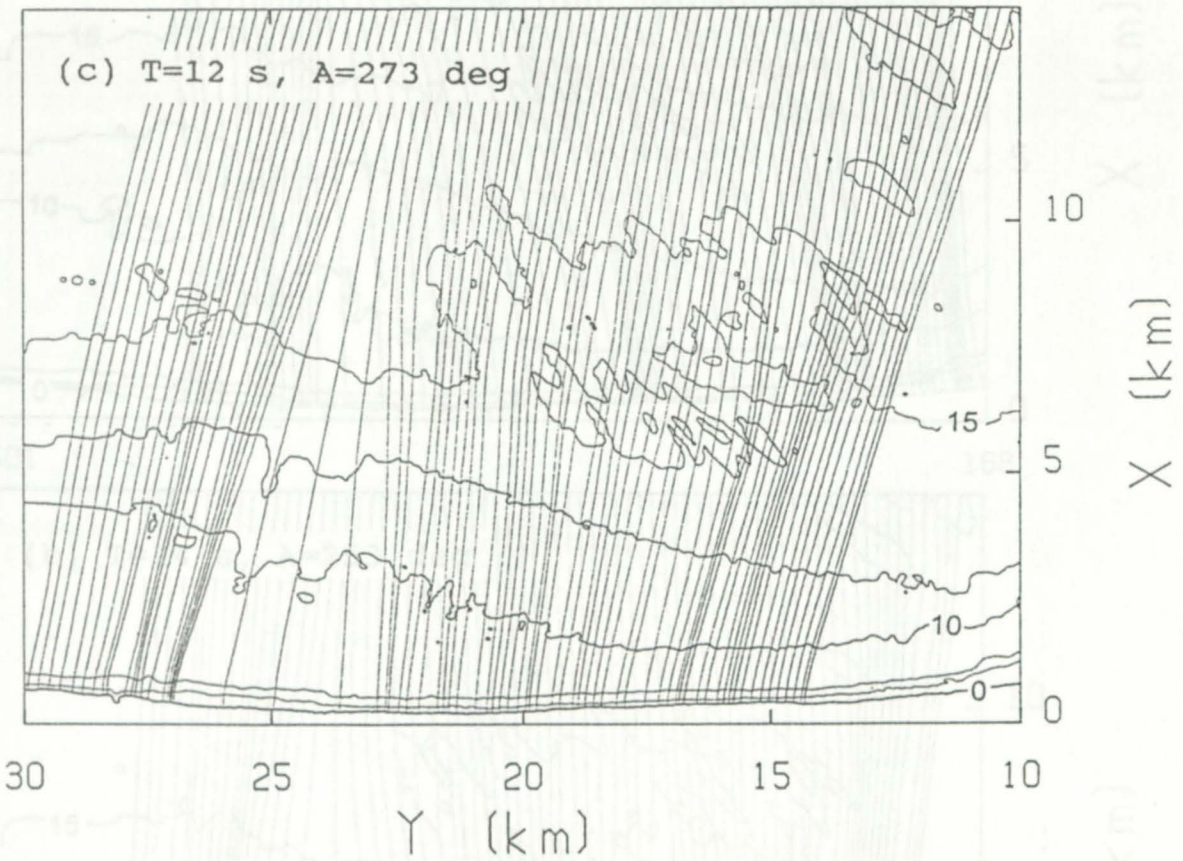

Figure 19c. Calculated wave rays for the Northeaster wave (H = 1.9 m, T = 12 s) for the existing bathymetry, waves approaching from the E (273°).

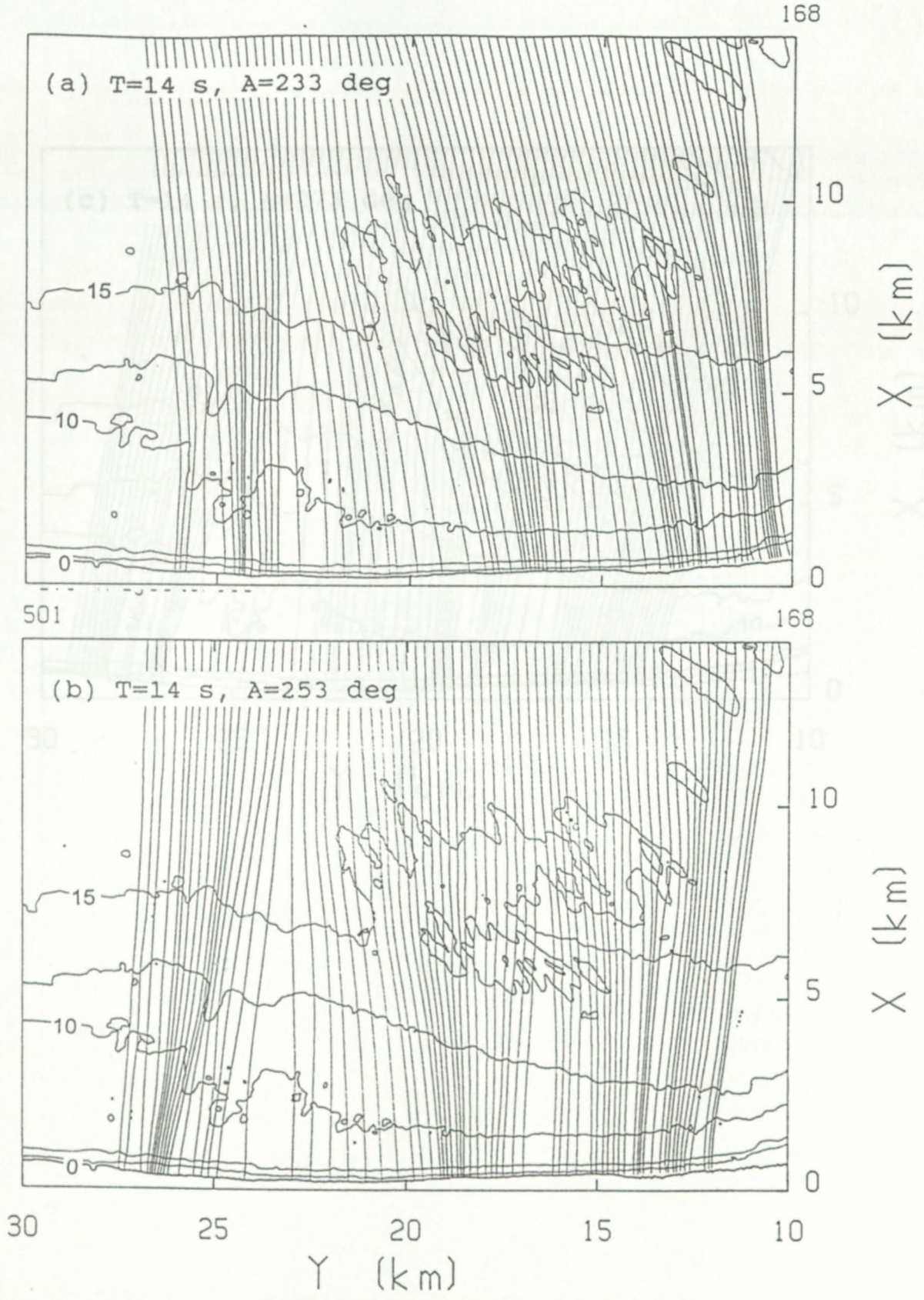

Figure 20. Calculated wave rays for the Severe Sea (H =3 m, T = 14 s) for the existing bathymetry. a) Waves approaching from the NE (233°). b) Waves approaching from the ENE (253°).

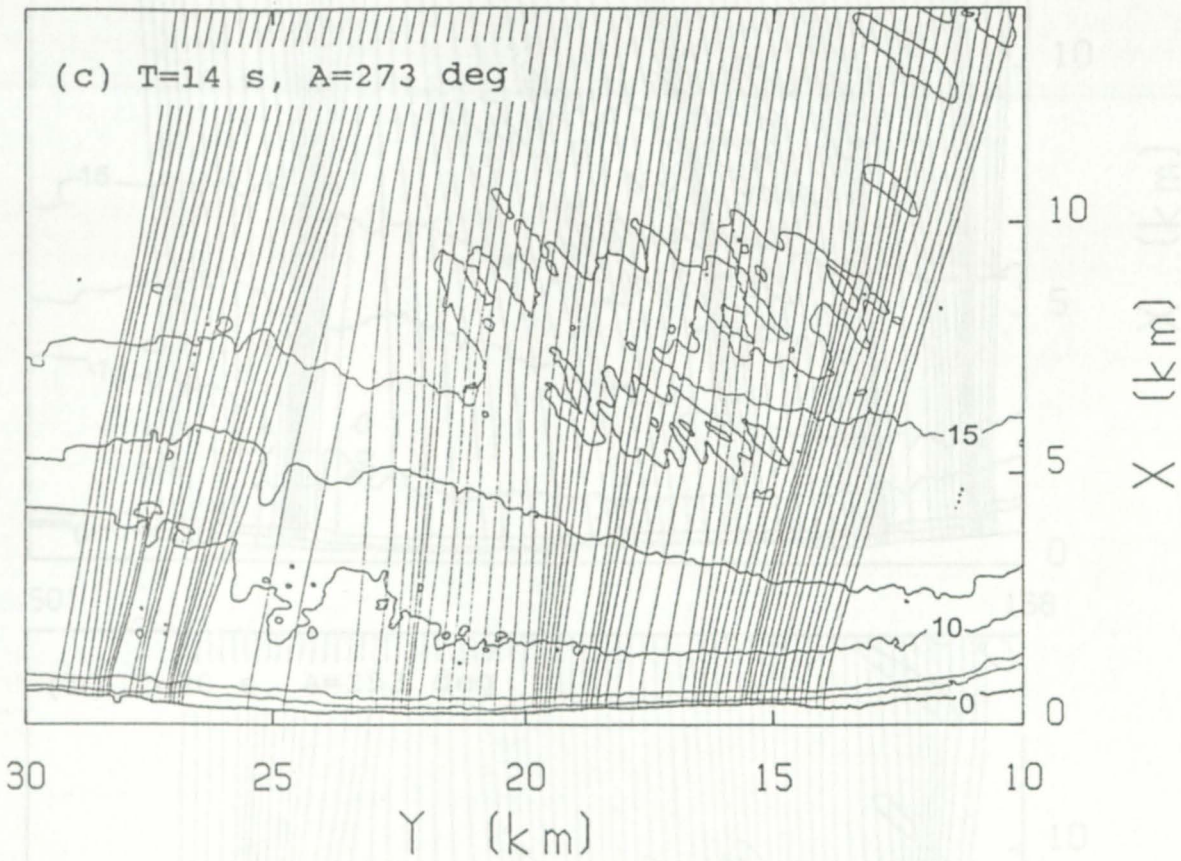

Figure 20c. Calculated wave rays for the Severe Sea (H = 3 m, T = 14 s) for the existing bathymetry, waves approaching from the E (273°).

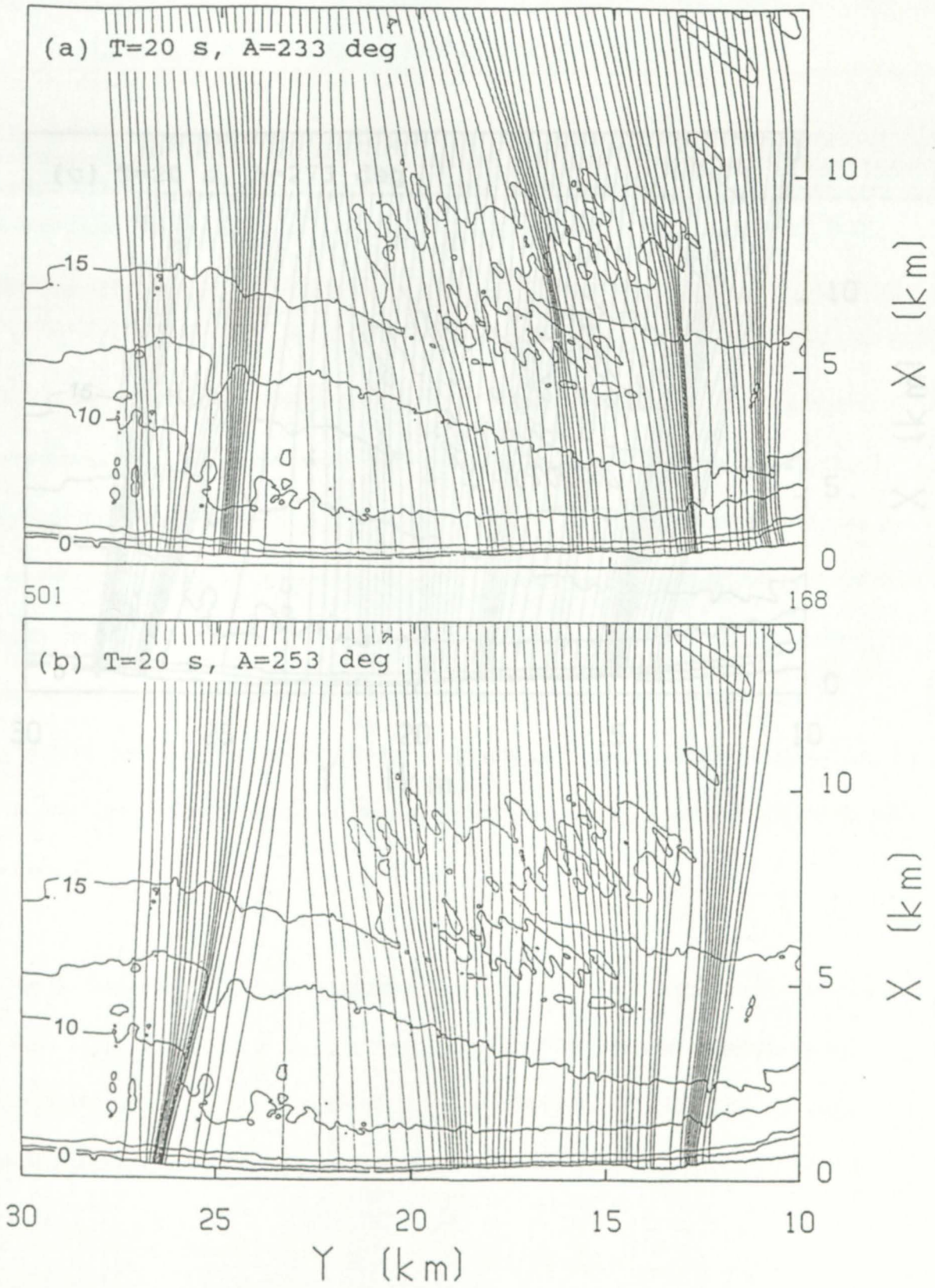

Figure 21. Calculated wave rays for the Most Severe Sea (H = 6.2 m, T = 20 s) for the existing bathymetry. a) Waves approaching from the NE (233°). b) Waves approaching from the ENE (253°).

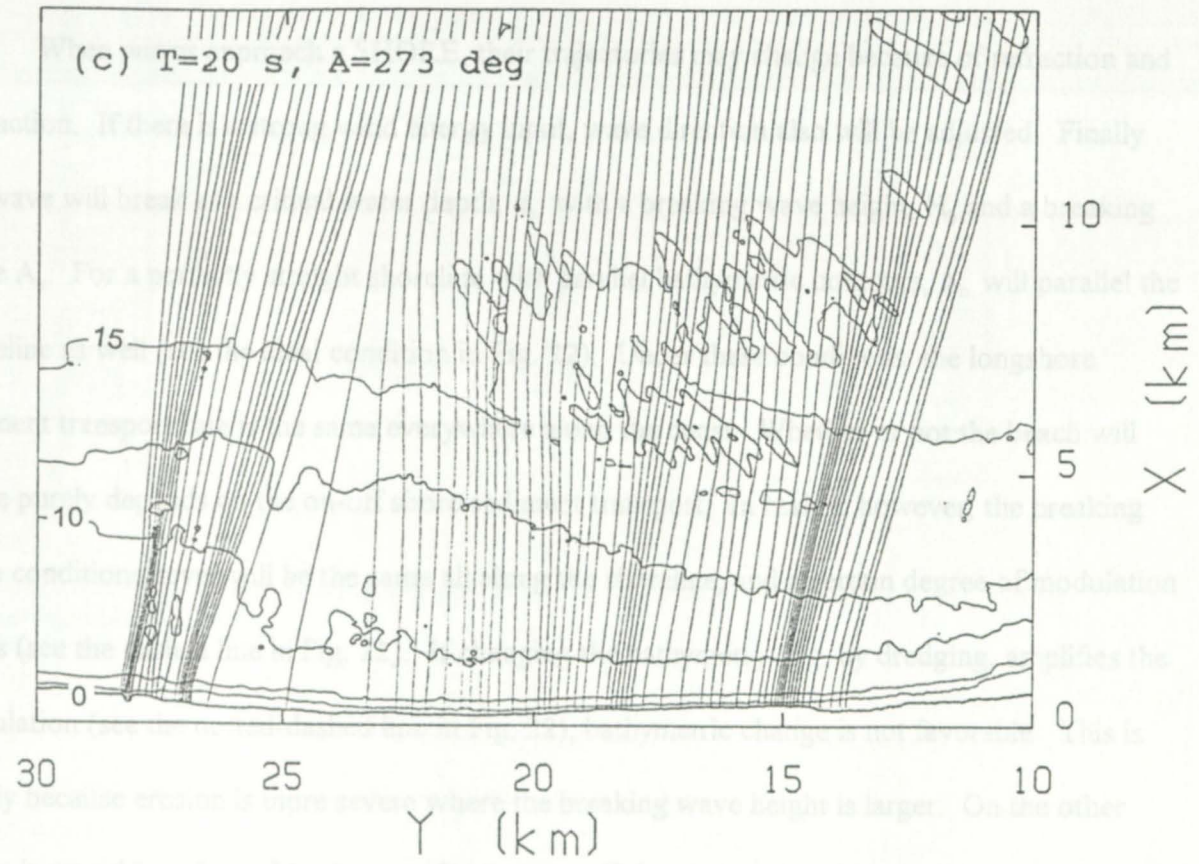

Figure 21c. Calculated wave rays for the Most Severe Sea (H = 6,2 m, T = 20 s) for the existing bathymetry, waves approaching from the E (273°).

CRITERIA FOR JUDGING THE INFLUENCE OF DREDGING

When waves approach a SHORE, their trajectories may change because of refraction and diffraction. If there is a strong wind energy input, wave direction also will be adjusted. Finally the wave will break at a critical water depth, d_b, with a breaking wave height, H_b and a breaking angle A_b. For a perfectly straight shoreline with parallel bathymetric contours, A_b will parallel the shoreline as well (see the ideal condition in Fig. 22). Under these conditions, the longshore sediment transport rate is the same everywhere along the coast. Whether or not the beach will erode purely depends on the on-off shore sediment transport. In reality, however, the breaking wave conditions never will be the same all along the shoreline, and a certain degree of modulation exists (see the dashed line in Fig. 22). If changing the bathymetry. *e.g.* by dredging, amplifies the modulation (see the dotted-dashed line in Fig. 22), bathymetric change is not favorable. This is simply because erosion is more severe where the breaking wave height is larger. On the other hand, it would be a favorable change of bathymetry if the modulation decreased (see the dotted line in Fig. 22).

In the evaluation of computing results given in the next section, we are using the original break wave height modulation as the base (thus, a number of 1). For a favorable change of bathymetry, the modulation should be reduced, i.e., less than 1.0 (*e.g.*, 0.5 in Fig. 22). Any change of bathymetry that increases the modulation (*e.g.*, 1.35 in Fig. 22) can be classified as unfavorable.

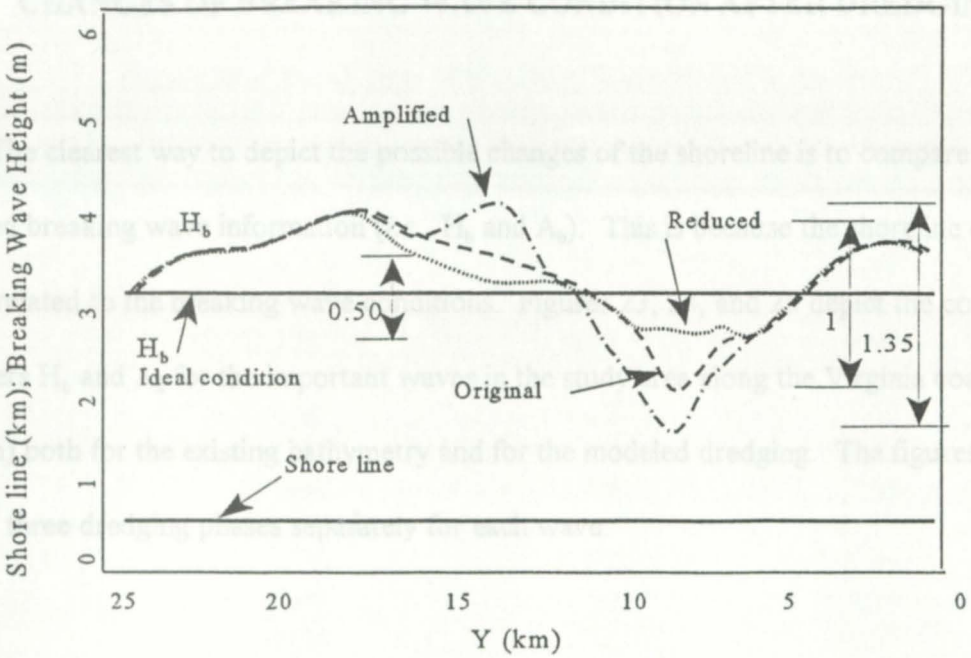

Fig. 22. A Conceptual Diagram Showing the Criterion for Determing the Effect of Bathymetric Change.

CHANGES OF BREAKING WAVE CONDITION AFTER DREDGING

The clearest way to depict the possible changes of the shoreline is to compare the calculated breaking wave information (*i.e.*, H_b and A_b). This is because the shoreline changes are directly related to the breaking wave conditions. Figures 23, 24, and 25 depict the computed parameters H_b and A_b for the important waves in the study area along the Virginia coast (y = 10 to 30 km) both for the existing bathymetry and for the modeled dredging. The figures show the plots for three dredging phases separately for each wave.

The calculated changes for the northeaster waves that propagate toward 233° (Fig. 23) indicate that the breaking wave height modulation increases a little (1.15) after the first phase of dredging. After the second phase, the modulation has a marginal increase (1.19). After the third phase, however, the modulation goes back to 1.0, an indication of no change at all for this particular wave condition. Table 6 summarizes the changes in breaking wave height modulation for the modeled wave conditions.

The data in Table 6 clearly show that after the completion of phase 1 dredging, all the five modeled wave directions and all the three wave conditions, demonstrate a negative impact on the breaking wave information (*i.e.*, all modulations are larger than 1). The worst case has an amplification ratio of about 330% (*i.e.*, 3.3). There is a little improvement after the completion of the second phase dredging although, for some cases, the situation becomes worse as the modulation is higher. Only after the completion of phase 3, does the situation improve significantly.

Table 6

Summary of the Change of Breaking Wave Height Modulation

Wave Dir.	Northeaster	Severe Sea	Most Severe Sea
233	1.15[1]	1.47	2.90
	1.19[2]	1.63	2.80
	1.00[3]	0.88	2.60
243	1.45	1.42	1.59
	1.27	1.37	1.47
	0.91	1.12	1.30
253	1.90	2.07	1.86
	1.40	1.30	1.50
	0.84	1.02	1.00
263	3.13	2.88	1.81
	2.0	2.90	2.43
	1.11	1.77	1.63
273	3.33	1.88	1.68
	2.70	1.70	1.77
	1.0	0.74	1.22

[1] indicates the completion of phase 1
[2] indicates the completion of phase 2.
[3] indicates the completion of phase 3.

For the northester waves, only one of the five wave directions (263°) has a slightly negative change (amplified modulation of 1.11). All other wave directions show either a positive (reduced modulation, *e.g.*, 0.84) or no change (modulation = 1).

The same conclusions can be made for the severe sea. The effects of dredging after the first and second phases are mainly negative. Only after the completion of the third phase are the

modeled impacts acceptable: waves that go toward 243° and 263° experience a small negative impact on the breaking wave height modulation. The 233° and 273° waves have a positive change, and the 253° waves appear to be unaffected by the dredging.

For the most severe sea, the possible impact after the completion of phase 1 and phase 2 are all negative. After the completion of phase 3, except for the normally incident waves (253°), waves coming from all other directions still experience a negative change. The worst scenario is for waves going toward 233° (coming from NE). A maximum change of breaking wave height modulation is more than 100%. For other directions, there are moderate increases of breaking wave height modulation (20% to 60%).

Notice that the most severe sea does not occur every year. More study on the prediction of this unfavorable sea is needed to estimate the possible wave direction for this sea condition. It is hard to estimate the possible impact of this rarely occurring event on the shoreline. Based on the results given in Table 6, only the most severe waves that go toward 233° cause a possible change of more than 100% in the breaking height modulation.

As was noted earlier, the RCPWAVE Model may over-predict the breaking wave height. Thus, the calculated 100% increase of breaking wave height modulation may also be an overestimate. Further study by using a more accurate model is necessary to provide a sound conclusion on the influence of this possible dredging.

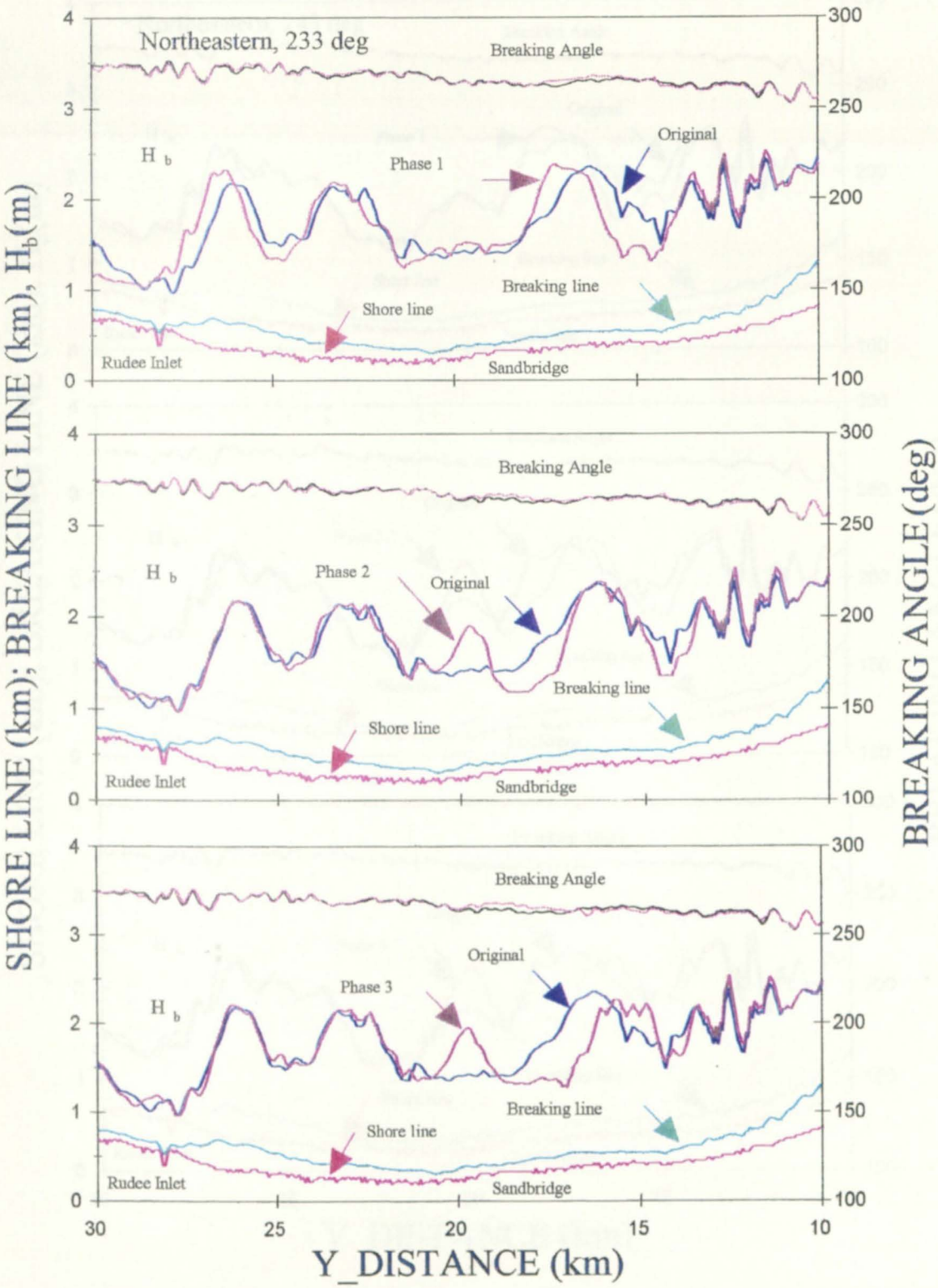

Figure 23. Changes resulting from phase 1, phase 2, and phase 3 dredging in breaking wave heights and angles for Northeaster waves from 233°.

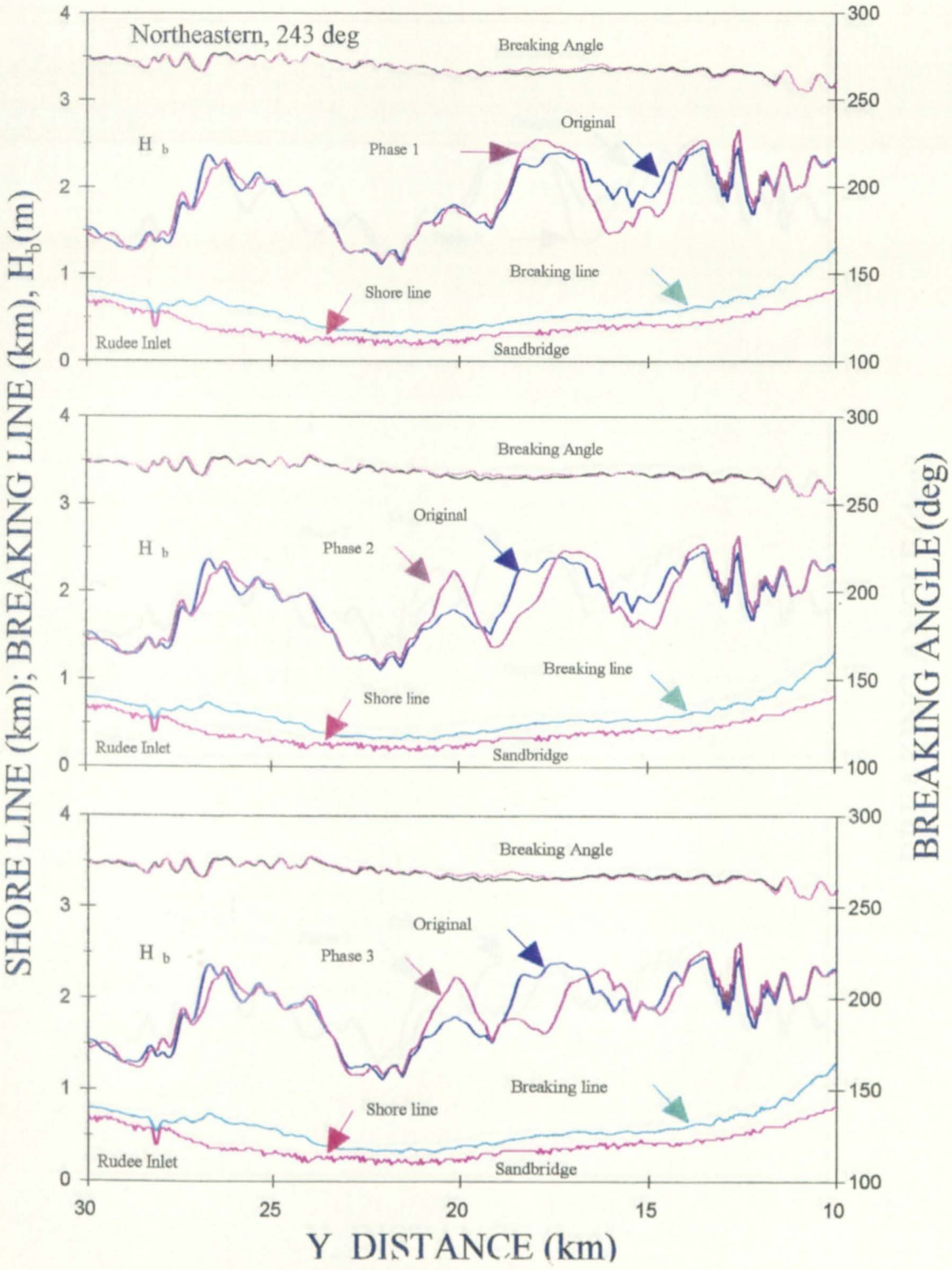

Figure 24. Changes resulting from phase 1, phase 2, and phase 3 dredging in breaking wave heights and angles for Northeaster waves from 243°.

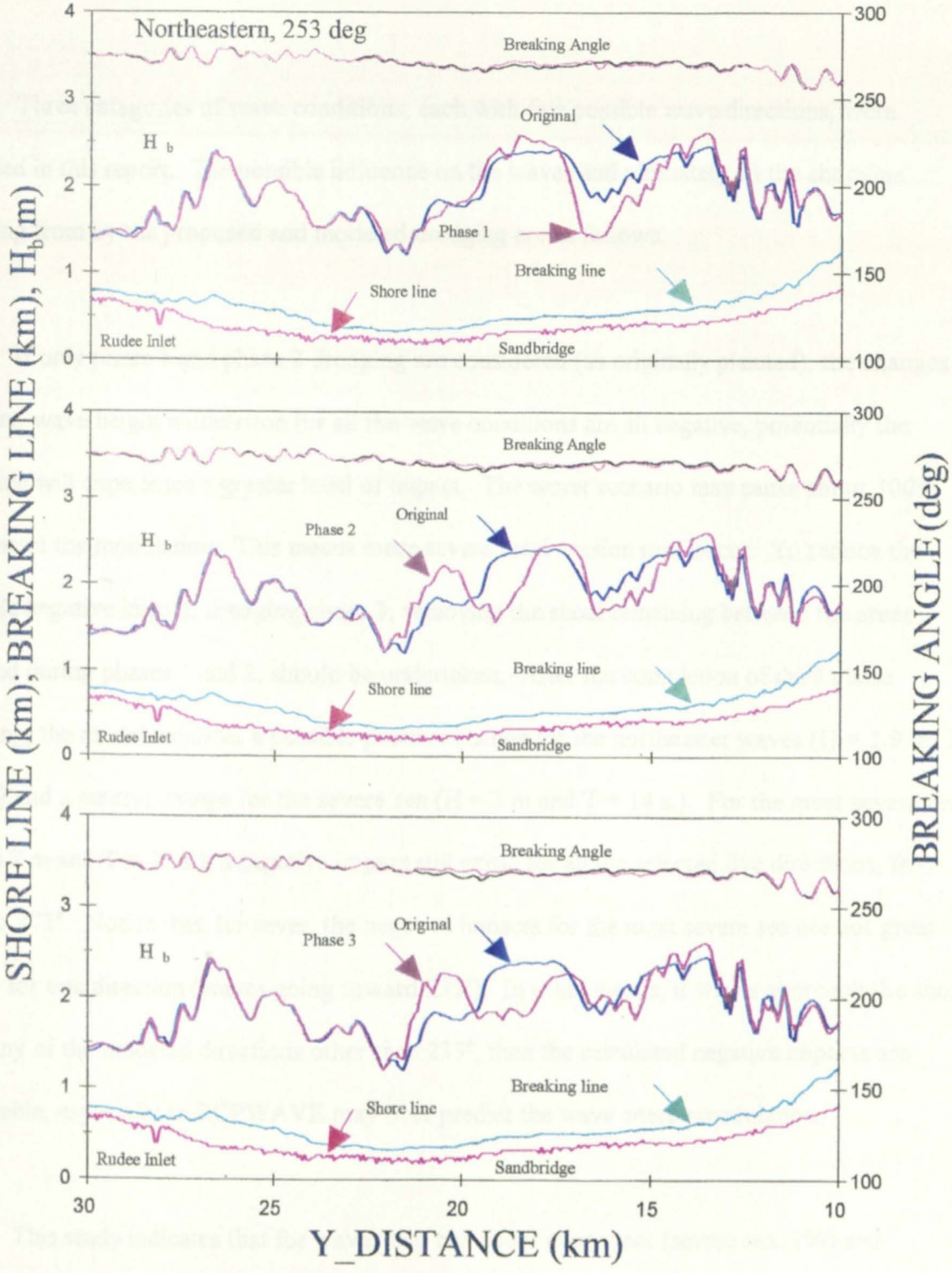

Figure 25. Changes resulting from phase 1, phase 2, and phase 3 dredging in breaking wave heights and angles for Northeaster waves from 253°.

CONCLUSIONS

Three categories of wave conditions, each with five possible wave directions, were modeled in this report. The possible influence on the waves and ultimately on the shoreline resulting from by the proposed and modeled dredging are as follows.

If only phase 1 and phase 2 dredging are considered (as originally planned), the changes in breaking wave height modulation for all the wave conditions are all negative, potentially the shoreline will experience a greater level of impact. The worst scenario may cause about 300% increase of the modulation. This means more severe local erosion may occur. To reduce the possible negative impact, dredging phase 3, removing the shoal remaining between the areas dredged during phases 1 and 2, should be undertaken. After the completion of third phase dredging, the model indicates a possible positive change for the northeaster waves (H = 1.9 m, T = 12 s) and a neutral change for the severe sea (H = 3 m and T = 14 s.). For the most severe sea (H = 6.2 m and T = 20 s.), a negative impact still exists for all the selected five directions, from 233° to 273°. Notice that, however, the negative impacts for the most severe sea are not great except for one direction (waves going toward 233°). In other words, if waves approach the shore from any of the modeled directions other than 233°, then the calculated negative impacts are reasonable, especially as RCPWAVE may over predict the wave energy modulation.

This study indicates that for waves that can occur every year (severe sea, 1%) and (northeaster, 5%), the revised dredging plan (sites A, B and C), if fully implemented, would not cause damage to the near-by beach. Local changes, however, still may exist. .

For the most severe sea, more studies to find the possible wave directions based on a reliable predictive model are needed for a better prediction of the possible effects of sand mining. This is because the most severe sea would only occur when a major storm or hurricane passed offshore of Sandbridge. Hurricane waves, however, are difficult to predict because hurricanes are fast, transient phenomena. The models that are currently available in the Far East for predicting typhoon waves should be used. The possibility of using the SWAN model (which is more suitable for slow moving wind fields) should also be examined.

The suggestion adding the third dredging area (site C, see Fig. 8) requires early communication with the authorities. The purposes of this communication would be to demonstrate the possible negative consequences of not implementing the third phase of dredging.

REFERENCES CITED

Berkhoff, J. C. W., 1972. Computation of Combined Refraction-Diffraction. Proceedings, 13th International Conf. on Coastal Engrg., ASCE, 1, 471-490.

Berkhoff, J. C. W., N. Booy, and A. C. Radder, 1982. Verification of Numerical Wave Propagation Models for Simple Harmonic Linear Water Waves. *Coastal Engrg.*, 6, 255-279.

Booij, N., L. H. Holthuijsen, and R.C. Ris, 1996. The SWAN wave model for shallow water. Proc. 25th Int. Conf. Coastal Engng., Orlando, USA, Vol. 1, pp. 668-676.

Booij, N., L.H. Holthuijsen and R. Padilla-Hernandez, in press. Wave propagation on a curvi-linear grid in a third-generation shallow water wave model. WAVES'97.

CERC, 1984. Shore Protection Manual, 4th Ed., U.S. Army Engineer Waterways Experiment Station, Coastal Engineering Research Center, Vicksburg, Miss.

Ebersole, B. A., 1985. Refraction-Diffraction Model for Linear Water Waves. *J. of Waterway, Port, Coastal, and Ocean Engrg.*, ASCE, 111(6), 939-953.

Goda, Y., T. Yoshimura, and M. Ito, 1971. Report of the Port and Harbor Research Institute. 10, (2).

Holthuijsen, L.H., N. Booij, R. Ris, J.H. Andorka Gal and J.C.M. de Jong, in press. A verification of the third-generation wave model "SWAN" along the southern North Sea coast. WAVES'97.

Holthuijsen, L.H., R.C. Ris, and N. Booij, in press. A verification of the third-generation wave model SWAN. 5th International Workshop on Wave Hindcasting and Forecasting, Jan. 27-30, 1998, Melbourne, Florida.

Kimball S. M. and J. K. Dame, 1989. Geotechnical Evaluation of Sand Resources on the Inner Shelf of Southern Virginia, Vol. 1: Report and Appendices A-B. Final Report to the City of Virginia Beach, Virginia, Virginia Institute of Marine Science, College of William & Mary, Gloucester Point, Virginia.

Kirby, J. T., and R. A. Dalrymple, 1991. User's Manual, Combined Refraction/Diffraction Model, REF/DIR 1, Version 2.3. Center for Applied Coastal Research, Dept. of Civil Engineering, Univ. of Delaware, Newark, Delaware, 19716.

Longuet-Higgins, M. S., D. E. Cartwright, and N. D. Smith, 1963. Observations of the Directional Spectrum of Sea Waves Using the Motions of a Floating Buoy. *In* Ocean Wave Spectra, Prentice-Hill, 111-136.

Maa, J. P-Y., 1995. Possible Impact of Dredging at Sandbridge Shoal. Project Report submitted to MMS on Investigations of Isolated Sand Shoals on the Inner Shelf of Virginia relative to the Potential for Aggregate Mining. Virginia Institute of Marine Science. Gloucester Point, Virginia 51.

Maa, J. P.-Y. and C.H. Hobbs, III, in press. Physical Impact of Waves on Adjacent Coasts Resulting from Dredging at Sandbridge Shoal, Virginia. *J. Coastal Research*

Maa, J. P.-Y, and H.-H. Hwung, A Wave Transformation Model for Harbor Planning. WAVES 97, Virginia Beach, VA, Nov. 4-6, 1997.

Massel, S. R., 1995, Ocean Surface Waves: Their Physics and Prediction World Scientific Publ., Singapore.

Meindl. E. A., and G. D. Hamilton, 1992. Programs of the National Data Buoy Center. *Bulletin of the American Meteorological Society*, 73(7), 985 - 993.

Radder, A.C., 1979. On the Parabolic Equation Method for Waterwave propagation. *J. Fluid Mechanics*, 95, 159-176.

Wright, L. D., C. S. Kim, C. S. Hardaway, S. M. Kimball, and M. O. Green, M.O., 1987. Shoreface and Beach Dynamics of the Coastal Region from Cape Henry to False Cape, Virginia. Technical Report, Virginia Institute of Marine Science, College of William & Mary, Gloucester Point, VA 23062.

APPENDIX

Calculated changes in breaking wave height and angle for the remaining modeled scenarios.

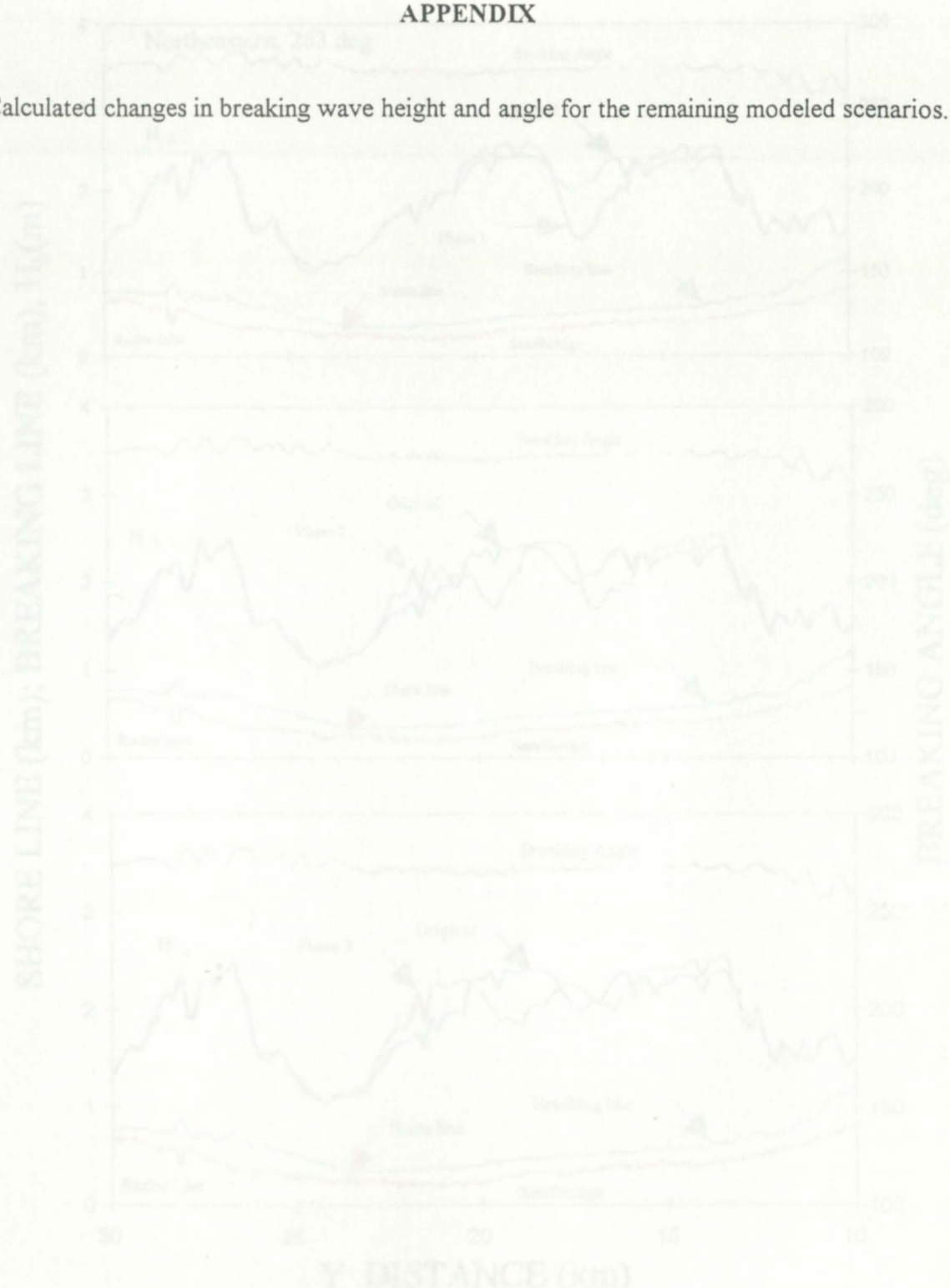

Figure 26. Changes in offset from plans 1, plans 2, and plans 3 displaying in breaking wave heights and angles for Northeaster waves from 203°.

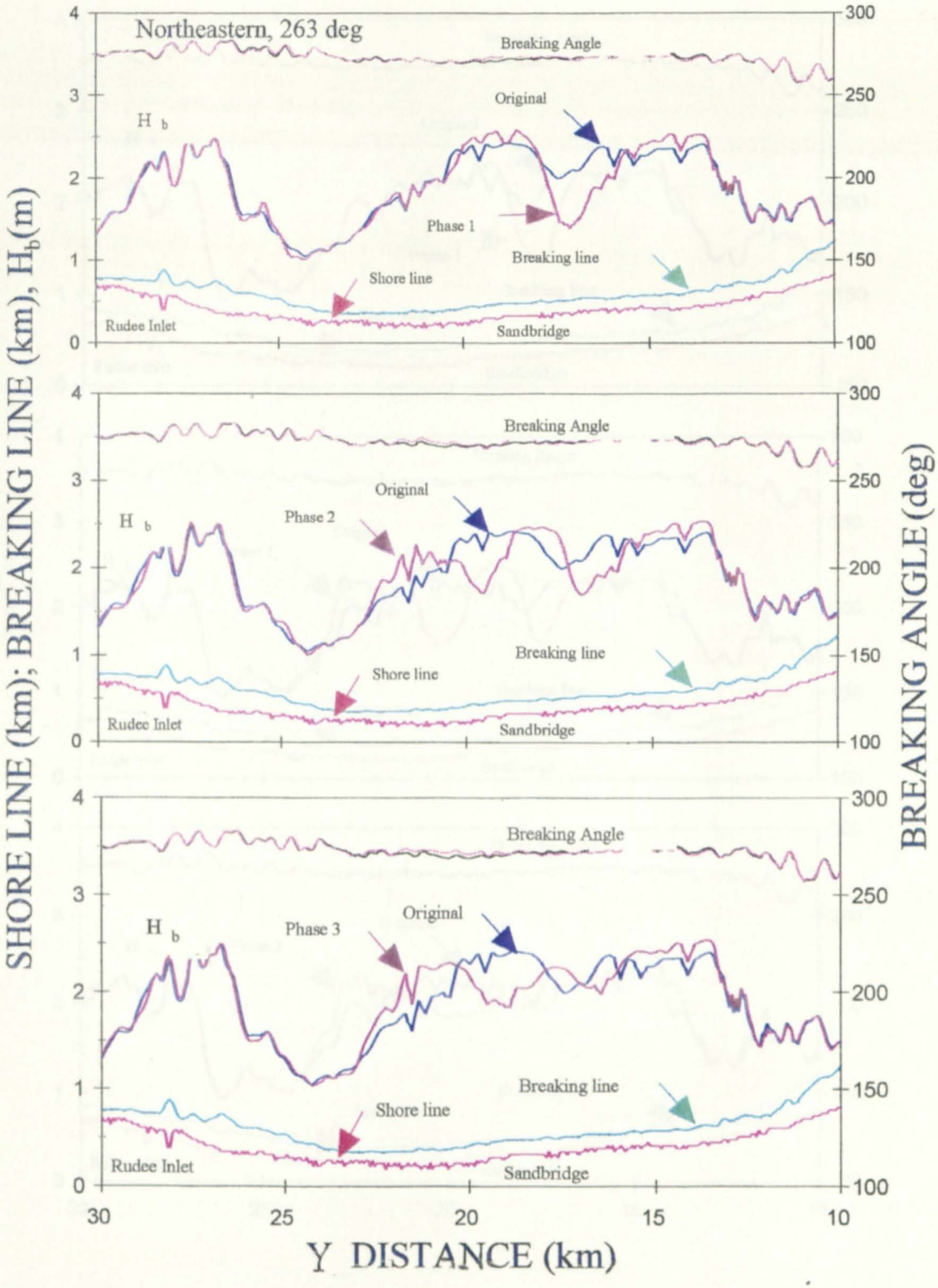

Figure 26. Changes resulting from phase 1, phase 2, and phase 3 dredging in breaking wave heights and angles for Northeaster waves from 263°.

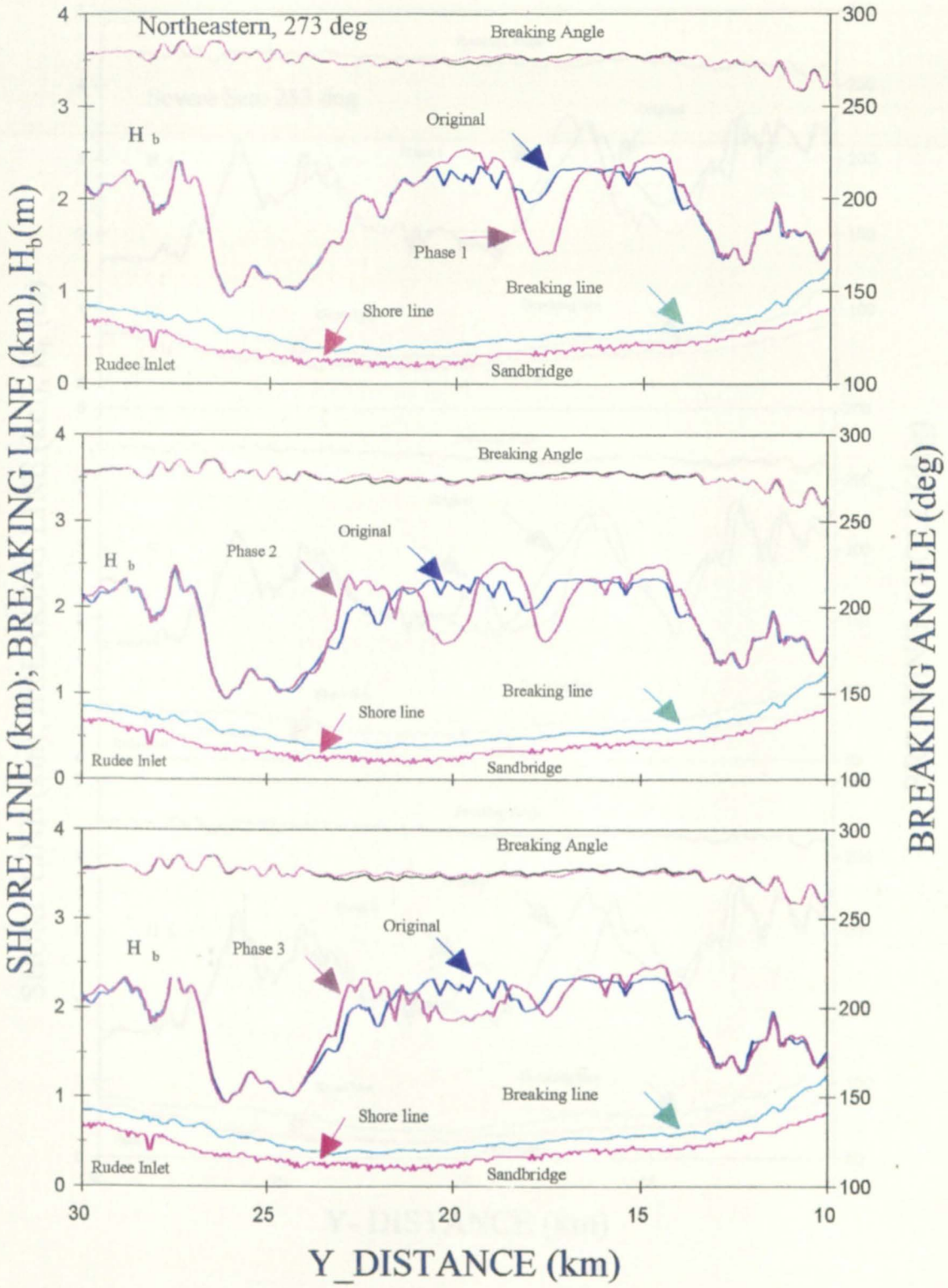

Figure 27. Changes resulting from phase 1, phase 2, and phase 3 dredging in breaking wave heights and angles for Northeaster waves from 273°.

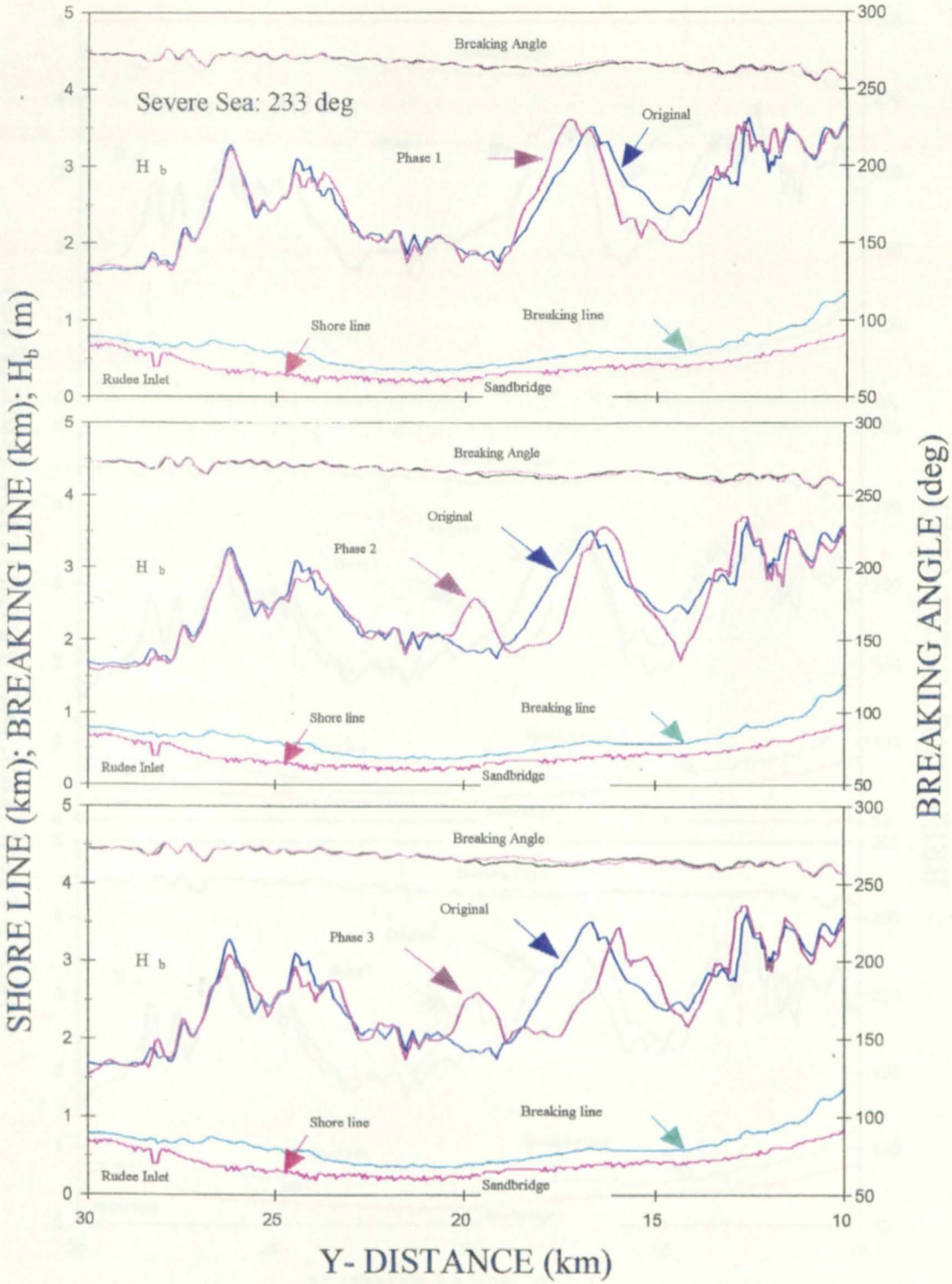

Figure 28. Changes resulting from phase 1, phase 2, and phase 3 dredging in breaking wave heights and angles for the severe sea from 233°.

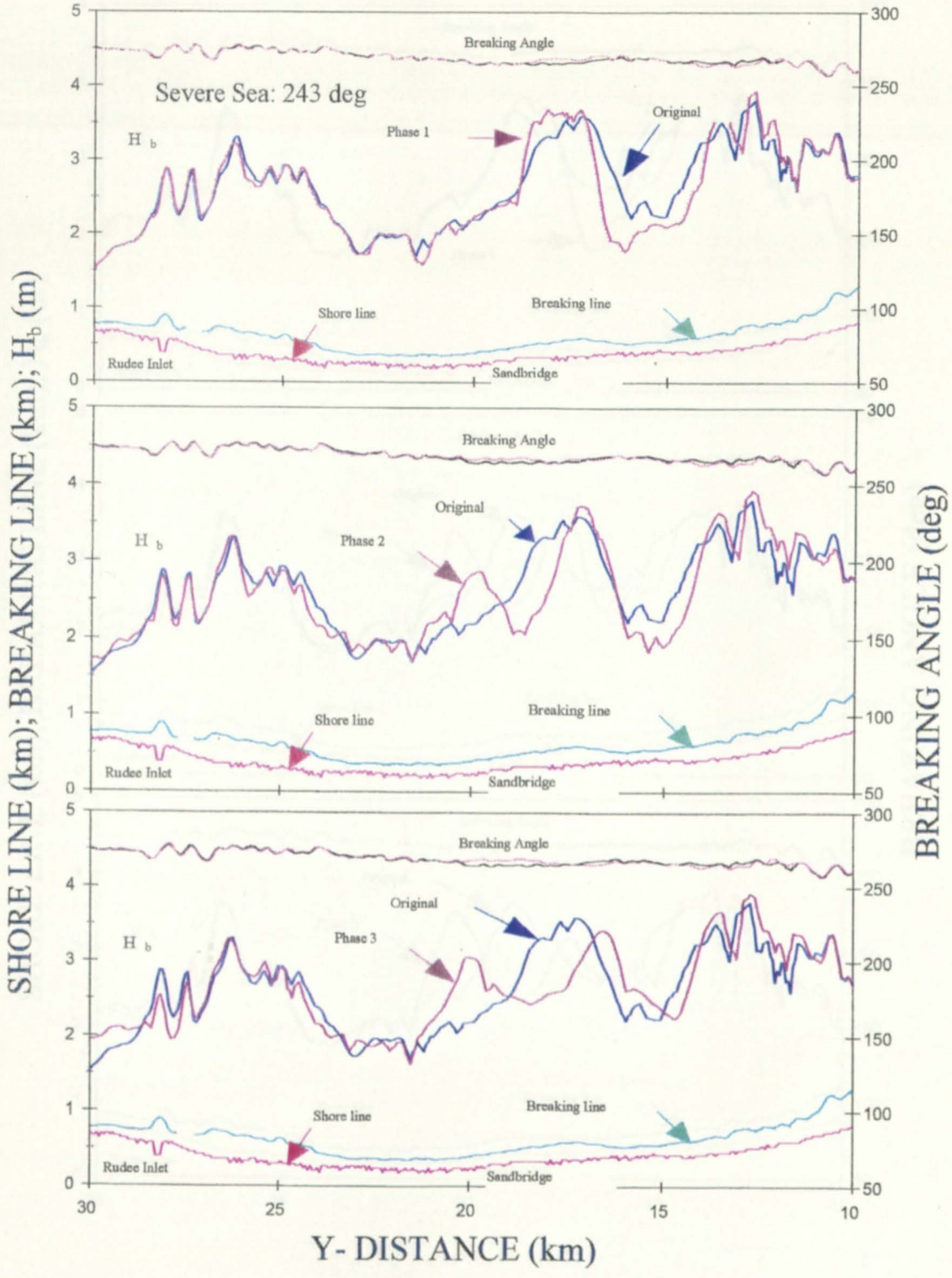

Figure 29. Changes resulting from phase 1, phase 2, and phase 3 dredging in breaking wave heights and angles for the severe sea from 243°.

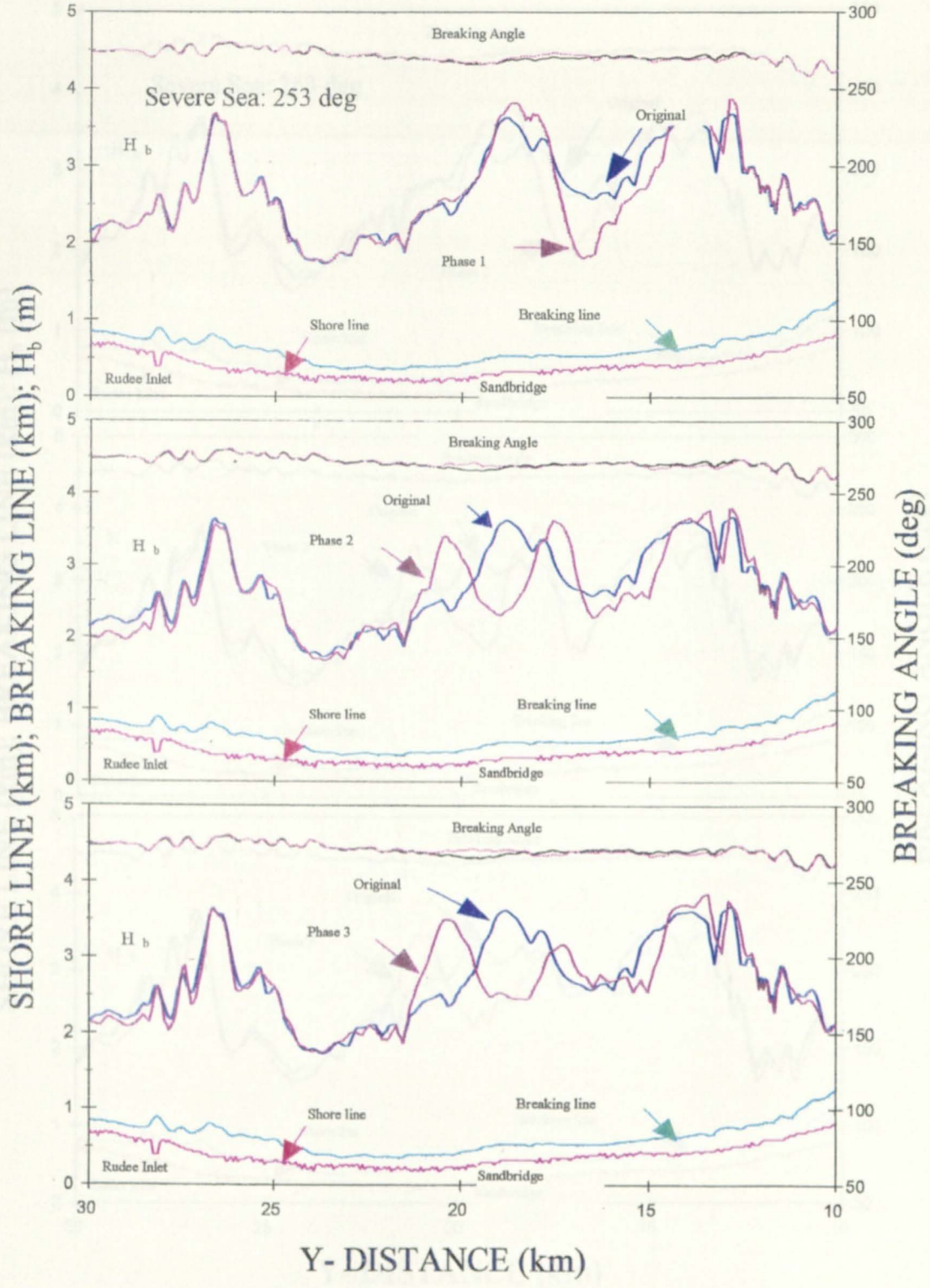

Figure 30. Changes resulting from phase 1, phase 2, and phase 3 dredging in breaking wave heights and angles for the severe sea from 253°.

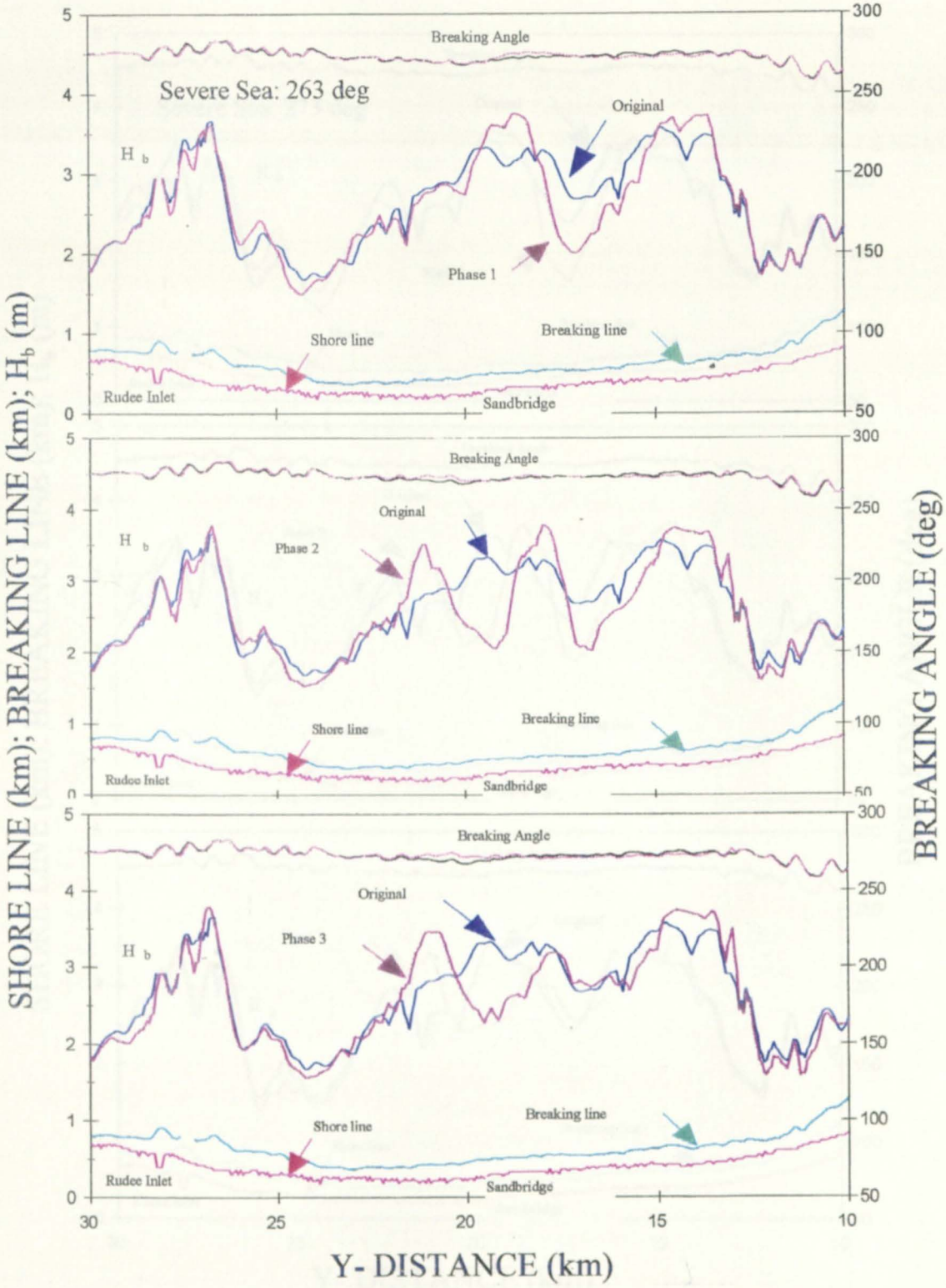

Figure 31. Changes resulting from phase 1, phase 2, and phase 3 dredging in breaking wave heights and angles for severe sea from 263°.

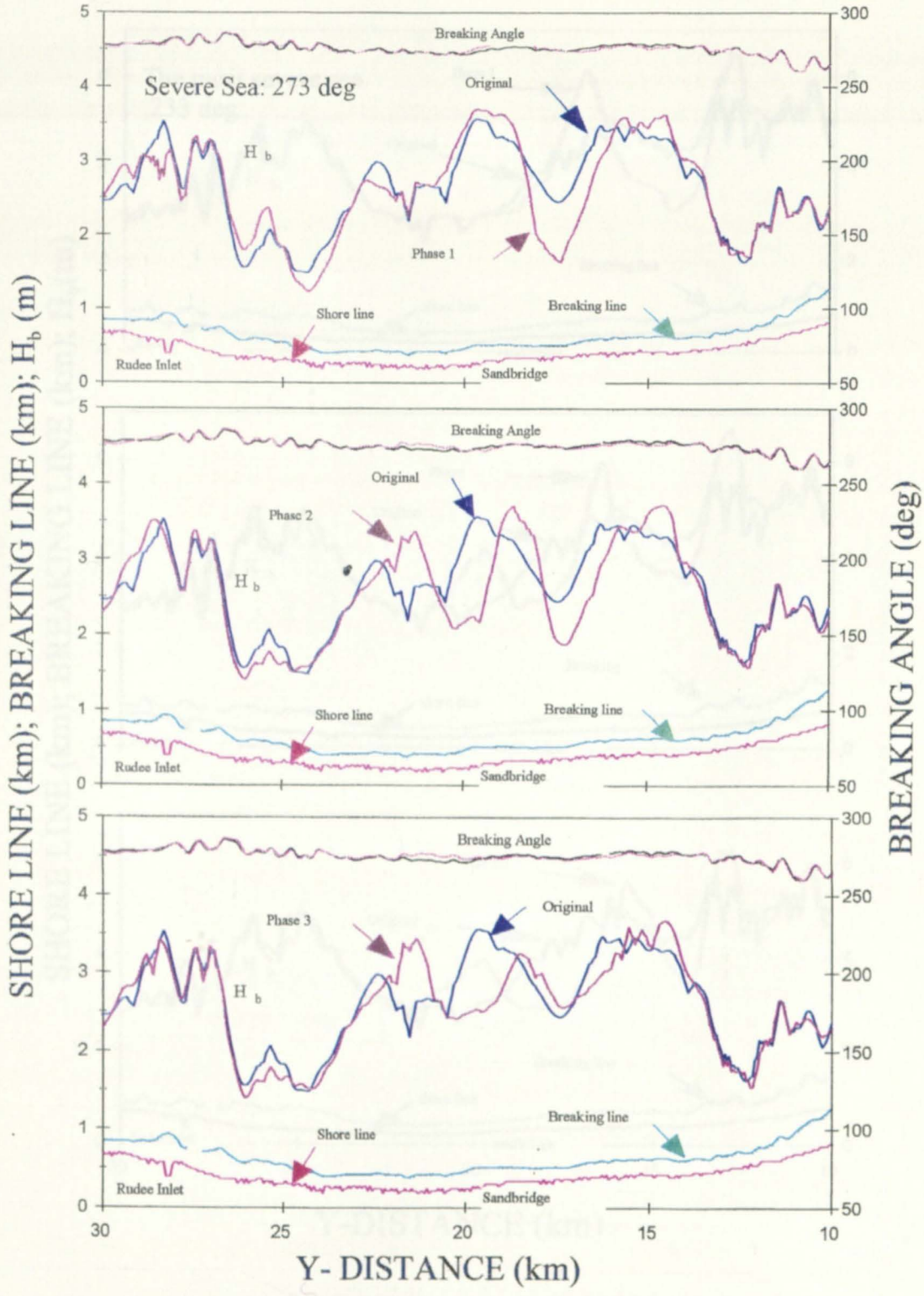

Figure 32. Changes resulting from phase 1, phase 2, and phase 3 dredging in breaking wave heights and angles for the severe sea from 273°.

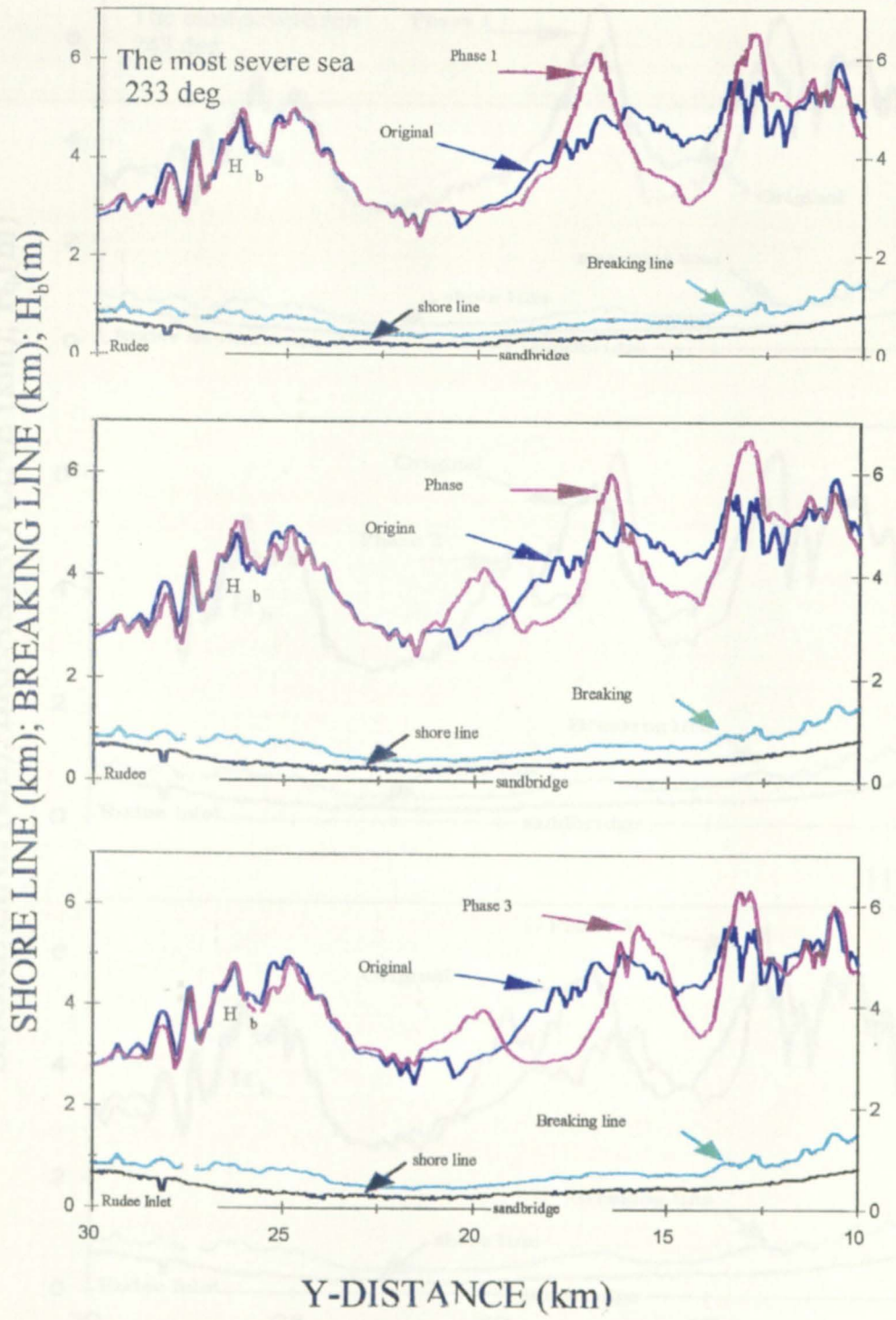

Figure 33. Changes resulting from phase 1, phase 2, and phase 3 dredging in breaking wave heights and angles for the most severe sea from 233°.

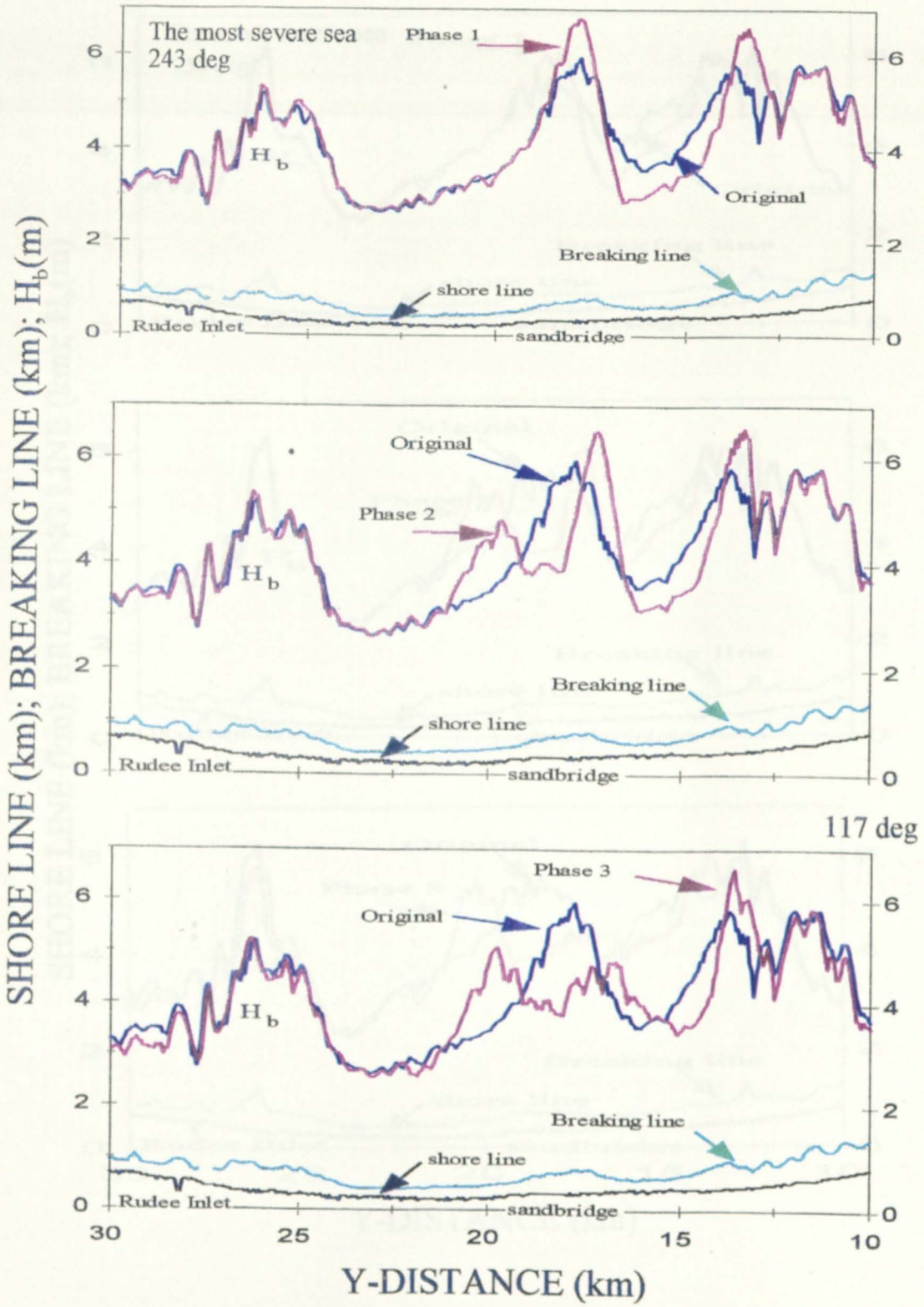

Figure 34. Changes resulting from phase 1, phase 2, and phase 3 dredging in breaking wave heights and angles for the most severe sea from 243°.

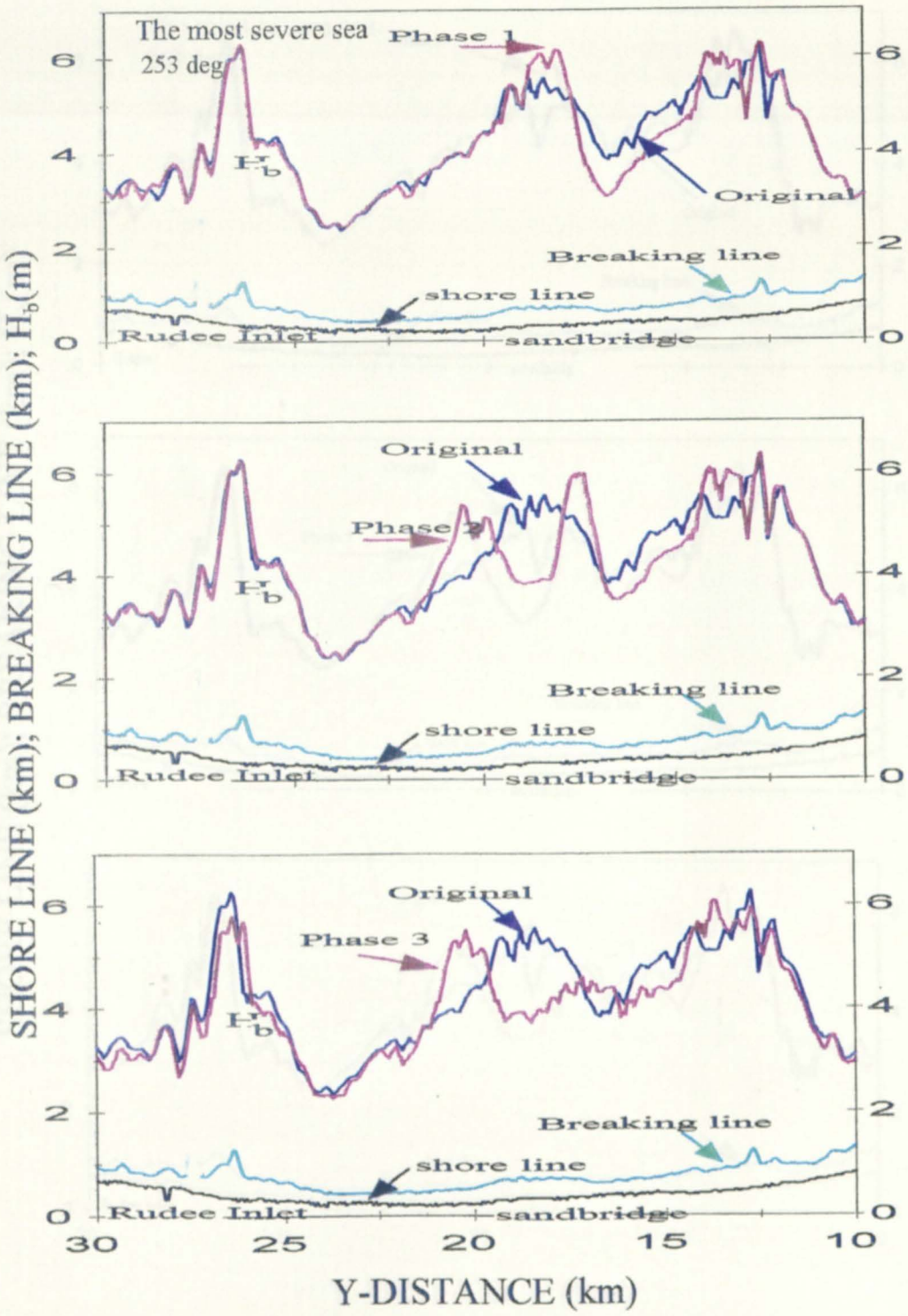

Figure 35. Changes resulting from phase 1, phase 2, and phase 3 dredging in breaking wave heights and angles for the most severe sea from 253°.

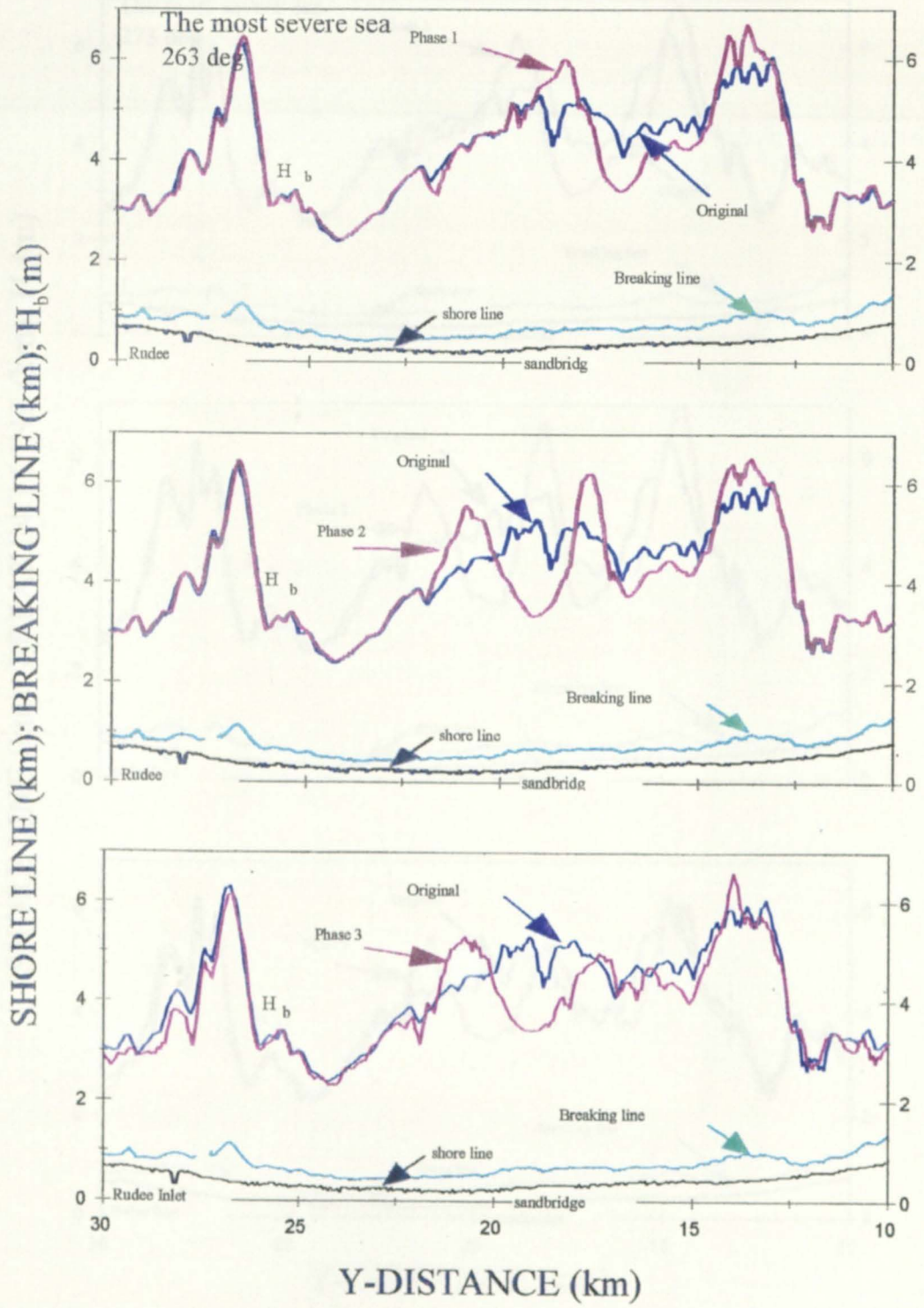

Figure 36. Changes resulting from phase 1, phase 2, and phase 3 dredging in breaking wave heights and angles for the most severe sea from 263°.

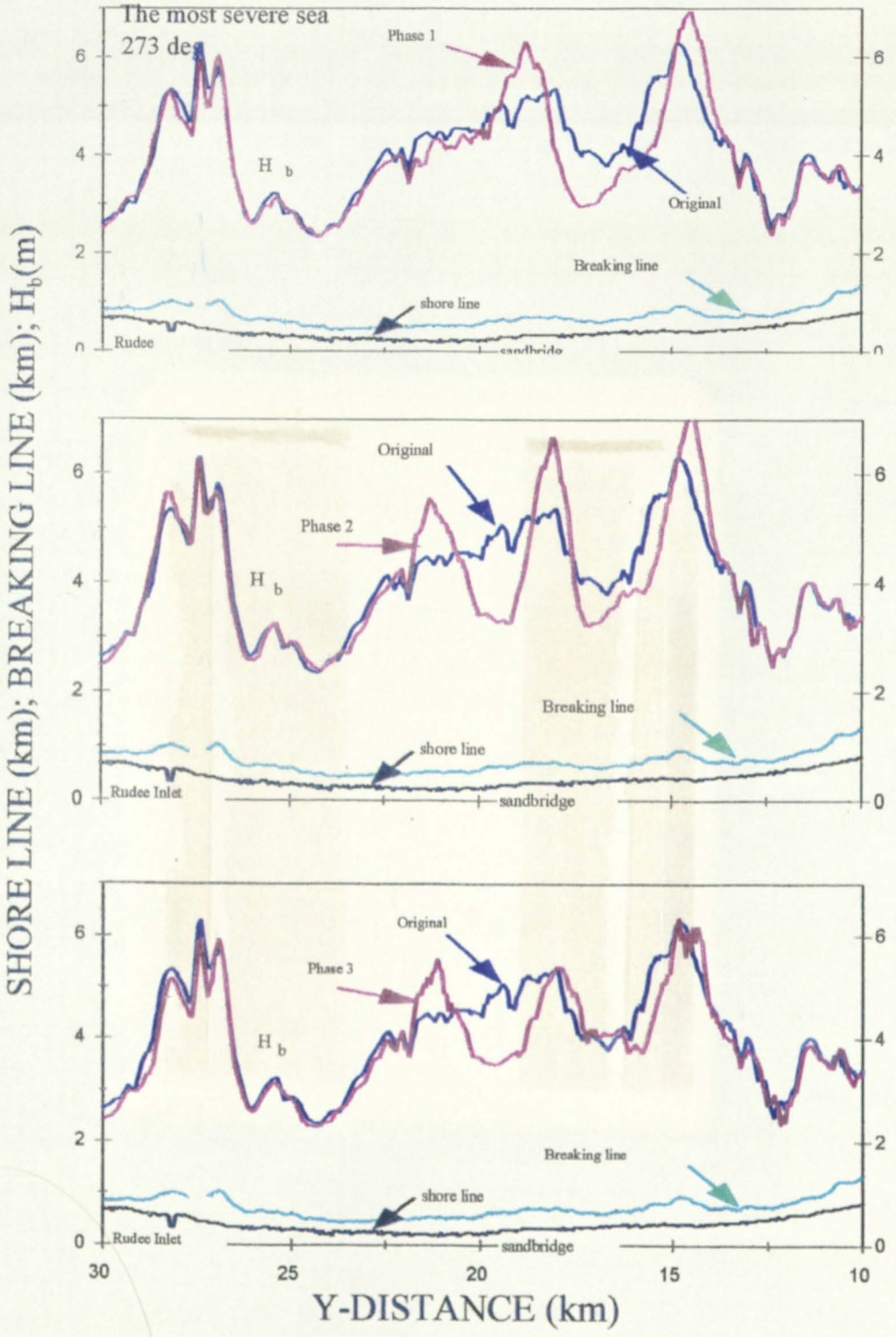

Figure 37. Changes resulting from phase 1, phase 2, and phase 3 dredging in breaking wave heights and angles for the most severe sea from 273°.